NACA

RESEARCH MEMORANDUM

EXPERIMENTAL INVESTIGATION OF AIR-COOLED TURBINE

BLADES IN TURBOJET ENGINE

IV - EFFECTS OF SPECIAL LEADING- AND TRAILING-EDGE

MODIFICATIONS ON BLADE TEMPERATURE

By Herman H. Ellerbrock, Jr., Charles F. Zalabak
and Gordon T. Smith

Lewis Flight Propulsion Laboratory
Cleveland, Ohio

NATIONAL ADVISORY COMMITTEE
FOR AERONAUTICS

WASHINGTON

April 13, 1951
Declassified December 11, 1953

NATIONAL ADVISORY COMMITTEE FOR AERONAUTICS

RESEARCH MEMORANDUM

EXPERIMENTAL INVESTIGATION OF AIR-COOLED TURBINE

BLADES IN TURBOJET ENGINE

IV - EFFECTS OF SPECIAL LEADING- AND

TRAILING-EDGE MODIFICATIONS ON BLADE TEMPERATURE

By Herman H. Ellerbrock, Jr., Charles F. Zalabak
and Gordon T. Smith

SUMMARY

An investigation is being conducted to determine experimentally the cooling effectiveness of a series of air-cooled blades in a production turbojet engine. This investigation has established that hollow blade shells with tubes and fins inserted in the coolant passages can be effectively cooled at the midchord regions. The leading and trailing edges were as much as 500° F higher than the midchord temperatures, however.

In order to reduce these high leading- and trailing-edge temperatures and thereby increase the allowable turbine-inlet temperatures, six blade configurations with special leading- and trailing-edge modifications were fabricated and investigated. These modifications appreciably reduced the chordwise temperature variations. At an engine speed of 10,000 rpm, an effective gas temperature of 1160° F, and a coolant- to gas-flow ratio of 0.056, the most effectively cooled blade had a maximum chordwise temperature variation of about 230° F as compared with 450° F for a blade with no special provision for cooling the leading and trailing edges of the blades. At these same conditions, the leading-edge, average midchord, and trailing-edge temperatures for the most effectively cooled blade were about 780°, 590°, and 740° F, respectively.

The leading-edge modifications in the order of increasing cooling effectiveness were (1) the increased leading-edge radius, (2) the herringbone slots, (3) the combination of increased leading-edge radius and a copper fin extending from the leading edge to a tube in the coolant passage, and (4) the combination of increased leading-edge

radius and radial slots. The trailing-edge modifications in order of increasing cooling effectiveness were (1) a radial groove in the pressure surface fed by 0.020-inch-diameter holes, (2) a radial groove on the pressure surface of the blade fed by 0.040-inch-diameter holes, (3) a copper fin extending through a split trailing edge to a tube in the coolant passage, and (4) radial slots.

The blades utilizing a reversal of coolant-flow direction at the blade tip required the greatest pressure drop to force a given amount of coolant through the blades; whereas the blade with a straight root-to-tip flow and herringbone slots required the least pressure drop. The blade with the copper fins in the leading- and trailing-edge regions exhibited a promising combination of strength, good cooling effectiveness, and low pressure drop.

INTRODUCTION

An investigation of a series of air-cooled turbine-blade configurations installed in a production turbojet engine is being conducted at the NACA Lewis laboratory with the principal objective of obtaining an air-cooled blade configuration that will satisfactorily operate at current turbine-inlet temperatures when the blades are fabricated from nonstrategic materials. Each blade configuration investigated is evaluated from data obtained from a pair of air-cooled blades installed diametrically opposite one another in place of two conventional uncooled blades in the turbine wheel of the turbojet engine.

Calculations based on the results obtained from the first three blade designs investigated (references 1 to 3) indicated that the high leading- and trailing-edge temperatures measured on these blade configurations may limit the operation of nonstrategic rotor blades to turbine-inlet temperatures considerably lower than those currently in use with uncooled blades of strategic material. Similar calculations based on the much cooler midchord blade temperatures indicated that nonstrategic blades could be operated well above the current inlet temperatures. In order to reduce these chordwise temperature gradients measured on the first three blades investigated and consequently to take advantage of the possible gains in turbine-inlet temperatures indicated by the calculations, six blade configurations having special modifications for cooling the leading and trailing edges were fabricated and investigated. The results obtained from the investigation of these six blade configurations are reported herein. The results of references 4 and 5 were used as a guide in designing a number of these cooled-blade configurations.

Because of blade stress limitations caused by thermocouple instal-
lation, the blade configurations were not investigated at rated engine
conditions but the temperatures and the cooling-air pressure-loss
results are indicative of the relative cooling merits of the different
blade configurations at the conditions of the investigation and also
serve to indicate what cooling performance might be expected at more
severe conditions of engine operation. The calculations on which the
estimates of allowable turbine-inlet temperatures were based considered
only the simple centrifugal stresses and stress-rupture data of the
proposed blade material. The thermal stresses imposed by the tempera-
ture gradients, vibratory stresses, stress redistribution caused by
plastic flow, and residual stresses were neglected in these calcula-
tions. In the final evaluation of any cooled-blade configuration for
design purposes, a more rigorous stress analysis taking into account
these stresses and systematic endurance testing is advisable. The
experiments were conducted over a range of coolant flow per blade from
about 0.01 to about 0.1 pound per second. The turbine-inlet tempera-
ture varied from about 960° F at 4000 rpm to about 1170° F at 10,000 rpm.

GENERAL PRINCIPLES OF COOLED-BLADE DESIGN

The design of cooled turbine blades for gas-turbine application
requires consideration of a variety of turbine-blade characteristics.
The principal blade characteristics requiring evaluation are blade
aerodynamics, blade stresses, blade-cooling performance, and the
interrelation among these characteristics.

Aerodynamic considerations will indicate a blade design that will
develop the required turbine work with the maximum obtainable aero-
dynamic efficiency. Blade-stress evaluation will involve consideration
of the centrifugal tensile stresses, centrifugal bending stresses, gas
bending stresses, thermal stresses, vibratory stresses, and the effects
of stress redistribution caused by plastic deformation. Additional
stress considerations that may require attention with specific blade
designs are the stresses induced by aerodynamic twisting and the
stresses resulting from the "unwrapping" tendency of twisted blade
designs. Residual stresses may also require evaluation. Centrifugal
tensile stresses, centrifugal bending stresses, and gas bending stresses
are well understood and the methods of evaluating them are standardized
(references 6 and 7). In cases where the gas bending stresses are
troublesome, the centrifugal bending stresses can be so controlled as

to eliminate or considerably reduce the gas bending stresses by location of the centroids of the blade cross sections on an appropriate nonradial line.

The thermal stresses can be calculated in the elastic-stress range (reference 8) and the influence of plastic deformation on the thermal stresses is considered in reference 9, but the vibratory stresses cannot, at present, be predicted with any certainty for design purposes. The combined action of all these stresses accompanied by plastic deformation produces blade stresses that can be evaluated only with simplifying assumptions, which seriously impair the reliability of the analysis. Systematic endurance testing of promising designs appears to offer the only means available at present for reliably evaluating the durability of a cooled-blade design.

The ideal cooling performance requires that the principal stress-carrying regions of the blade be cooled to a minimum temperature by a minimum of coolant flow. Such a cooled blade may not be entirely devoid of chordwise temperature gradients because certain regions of the blade are inherently difficult to cool. Reducing the temperatures of these parts of the blade to the temperatures of the more easily cooled regions may require an uneconomical expenditure of coolant, which could be better utilized to further reduce the temperatures of the more easily cooled regions of the blades. Ordinarily, the requirements of stress and aerodynamics determine the blade design. The interrelation of the cooling requirements with those of stress and aerodynamics may result in a modification of the blade design dictated by the usual considerations of stress and aerodynamics alone. Blades may require thicker cross sections in order to accommodate the required coolant passages. Shorter, more rounded leading and trailing edges may be desirable in order to improve the cooling effectiveness in these regions.

A reduction in blade temperature can be accomplished by increasing the gas-to-blade heat-transfer resistance and decreasing the heat-transfer resistance through the blade wall and from the blade wall to the coolant.

The increase in gas-to-blade heat-transfer resistance can be accomplished by reducing the gas temperature in the neighborhood

of the blade wall and by reducing the gas-to-blade heat-transfer
coefficient. The reduction of the gas temperature in the neighbor-
hood of the blade can be effected by bleeding a film of cooling
air from the inside of the blade through slots in the blade shell.
The reduction of the outside heat-transfer coefficient in the
vicinity of the stagnation point can be accomplished by properly
shaping the blade profile. It is shown in reference 10 that the
heat-transfer coefficient in this region is proportional to $\sqrt{1/x}$,
where x is the radius of curvature of the leading edge of the
blade. Because the heat-transfer coefficient near the leading
edge of the blade is very large, the radius of curvature of this
portion of the blade is an important cooled-blade design considera-
tion.

The resistance to heat transfer by conduction through the
blade walls can be minimized by the use of high-conductivity mater-
ials. Unfortunately, high-conductivity materials do not have
sufficient strength at proposed cooled-blade operating tempera-
tures and consequently must be partially supported by some other
high-strength material.

An additional design consideration is the cooling-air pres-
sure loss in the coolant passages. This loss should be small
enough that the required coolant-flow rate can be provided by
the compressor discharge pressure; additional gains in cycle
efficiency may result from still further reducing the coolant
pressure loss.

BLADE MODIFICATIONS

As has been previously pointed out, the first blade config-
urations investigated were adequately cooled at the midchord
positions but were much hotter at the leading and trailing edges.
In order to reduce these gradients, six cooled-blade configura-
tions, hereinafter designated blades 4, 5, 6, 7, 8, and 9, were
fabricated and investigated.

Blade 4

The first of these blades to be investigated, blade 4, had the
leading-edge radius increased from about 0.05 inch to about 0.099
inch (approximately doubled). This increase in leading-edge radius
will result in a decrease in the outside heat-transfer coefficient,
as was previously discussed. According to the relation mentioned,
an effective gas temperature of 1200° F, and for a ratio of inside
coefficient to outside coefficient of 0.2, doubling the leading-edge
radius should reduce the blade temperature in this region about 65° F.
The aerodynamic effects of increasing the leading-edge radius may be
detrimental at high Mach numbers but may also have the effect of
improving off-design-point performance. The trailing edge of blade 4
was modified by drilling 26, 0.020-inch holes located 0.125 inch apart
in a radial gooove that was cut on the pressure surface of the blade
near the trailing edge (fig. 1(a)). Cascade investigations (refer-
ence 11) indicated that the groove would provide sufficient radial
distribution of the cooling air to cover the entire pressure surface
along the trailing edge of the blade, thus forming an insulating
layer of cool air on the outside pressure surface of the blade trail-
ing edge. The interior of blade 4 was packed with 30 stainless-steel
tubes; 28 of the tubes had a 0.090-inch outside diameter and a
0.0125-inch wall thickness, the tube nearest the leading edge had a
0.156-inch outside diameter and a 0.020-inch wall thickness, and the
tube nearest the trailing edge had a 0.125-inch outside diameter and
a 0.018-inch wall thickness. The passage formed by the outside wall
of the rearmost tube and the shell interior was capped at the tip so
that the cooling air in this passage would flow through the 0.020-inch-
diameter holes to form the protective film on the pressure surface of
the blade.

Blade 5

The next blade to be investigated was identical to blade 4 except
that seven tubes along the mean camber line were plugged with 1600° F
eutectic solder (fig. 1(c)). The purpose of this change was to evaluate
the gains in cooling effectiveness that might be achieved by confining
the cooling air to the tubes immediately adjacent to the blade wall.
A future method of blade design employing a comparatively cool solid-
center member carrying the load of the tubes and the shell might be
indicated if the cooling effectiveness were improved.

Blade 6

Blade 6 had the leading edge modified by cutting herringbone slots 0.0105 inch in width and 0.25 inch in length at an angle of 45° to the leading edge to provide the insulating layer of cooling air around the leading-edge regions of the blade (fig. 2). The trailing edge was the same as the trailing edges of blades 4 and 5 except that the holes were 0.040 inch in diameter. The center portion of the blade was packed with six SAE 1015 steel tubes of 0.156-inch diameter and 0.020-inch wall thickness and four stainless-steel tubes of 0.125-inch outside diameter and 0.018-inch wall thickness. The leading- and trailing-edge passages were capped at the blade tip, thus forcing the cooling air in these passages to flow through the slots and the holes.

Blades 7 and 8

The next two blade configurations investigated are shown in figure 3. The design of these blades attempted to make use of the natural-convection effects previously mentioned to augment the forced-convection flow and, in addition, to provide improved film cooling of the leading- and trailing-edge regions by the use of radial slots for bleeding the cooling air from the blade interior to the outside surface of the blade wall. In order to effect the tip-to-root flow in the leading- and trailing-edge regions of the blade, the entire tip of the blade was capped and seven tubes were brazed into the midchord portion of the shell so that they terminated about 0.25 inch from the capped tip. Cooling air was introduced exclusively through these tubes and flowed radially outward into the space between the blade cap and the tube ends. The air then reversed direction and flowed radially inward in the leading- and trailing-edge regions of the blade. The leading edge was modified by having an increased leading-edge radius and three rows of radial slots. The trailing-edge pressure surface was ground away except for two small supporting struts so that a radial slot for providing a film coverage of the trailing edge resulted. As the cooling air flowed radially inward in the leading- and trailing-edge passages, it also flowed out through the slots, thus forming a cool film of air on both the leading- and trailing-edge regions of the blades.

Seven tubes were located in the midchord region of the blade. Four of these tubes were SAE 1015 steel and had an outside diameter of 0.156 inch. The remaining three tubes were of stainless steel and had an outside diameter of 0.125 inch. All tubes had an 0.020-inch wall thickness.

The results obtained from the investigation of blade 7 indicated that the supporting struts in the trailing-edge slots caused an

undesirably severe temperature gradient in the vicinity of the strut, presumably resulting from the interruption of and turbulence induced in the film of cooling air. This interruption and turbulence in the film of coolant decrease the resistance to heat transfer to the trailing edge and consequently result in a high-temperature region immediately behind the strut. Blade 8 was identical to blade 7 except that one of the supporting struts in the trailing-edge radial slot was removed.

Blade 9

The practicability of utilizing high-conductivity materials to reduce the chordwise temperature gradients by conduction was investigated with blade 9 (fig. 4). The leading edge of blade 9 was modified, in addition to increasing the leading-edge radius, by brazing a 0.025-inch thick copper fin to the inside surface of the leading edge and to the first of seven copper tubes packed in the midchord region of the blade. Copper tubes were used in the midchord region of the blade in order to evaluate the cooling improvements obtainable by increasing the conductivity of the finning in the coolant passages. Four of these tubes were of 0.187-inch outside diameter and three were of 0.125-inch outside diameter. All tubes had an 0.032-inch wall thickness.

The trailing edge was modified by grinding a 0.025-inch radial slot, which split the trailing edge, and brazing into this slot a copper fin, which extended from the outside surface of the trailing edge through the slot to the rearmost tube of the copper tubes packed in the blade-coolant passage. The air-flow path was from the blade root to the blade tip.

A summary of the geometric characteristics of each blade configuration is presented in table I.

APPARATUS AND INSTRUMENTATION

Engine

A number of production turbojet engines were modified to accomodate and to supply cooling air to a pair of diametrically opposed air-cooled turbine blades. The modifications to the engines were the same as those described in detail in reference 1. The engine and the coolant-flow measurements and instrumentation were also the same as described in references 1 and 2.

Air-Cooled Blades

The cooled blades previously described were instrumented so that a peripheral-temperature distribution at approximately the one-third-span position and a radial-temperature distribution near the trailing edge could be obtained. Provisions were also made for measuring the cooling-air inlet temperature at the base of each cooled blade and the temperature of an uncooled blade adjacent to each cooled blade. The locations of the thermocouples used to provide the temperature profiles described are shown in figure 5. It will be noted that the temperature at the extreme leading edge, one-third-span position on the cooled blade, was not measured on blades 7 and 8 but was relocated on the midchord pressure-surface position indicated by Q in figure 5(c). This relocation was made in order to determine the temperature at a location where it was expected to be high. The other slight differences in thermocouple locations from one cooled blade to another were necessitated by the configurations of the blades. For example, the small radial deviation of the leading-edge thermocouple of blade 6 from the locations of similar thermocouples on the other blades was necessitated in order to locate the leading-edge thermocouples midway between the herringbone slots of blade 6.

PROCEDURES

Test

The procedure for conducting these investigations was the same as that for the first blade investigated (reference 1). In general, several series of runs were made at a number of engine speeds for each cooled-blade configuration. At each engine speed, the cooling-air flow was varied over a range of flows by manually controlled valves in the supply line. At the beginning of each blade investigation, a run was made to determine whether the cooling air was being equally distributed to each of the two cooled blades. This check was made by noting the temperatures of the cooled blades and the cooling-air inlet temperatures at identical locations on each of the cooled blades. The test conditions for the main series of runs on each blade are given in table II.

Calculation

Blade-temperature comparisons. - The calculation procedures for correlating the cooled-blade temperatures are developed in reference 1

and have been used to correlate the results of the present investigation. This method is based on the approximation that

$$\varphi = f(w_a, w_g) \tag{1}$$

where f denotes "function of" and

$$\varphi = \frac{T_{g,e} - T_B}{T_{g,e} - T_{a,e,h}} \tag{2}$$

In order to compare the temperature distributions on different blades of this and previous investigations at a set of common effective gas and cooling-air temperatures, cooled-blade temperatures had to be calculated at conditions slightly different from those under which these blades were investigated. The method of accomplishing this adjustment is described in detail in reference 2, which permits calculation of the blade temperature for specific values of $T_{a,e,h}$ and $T_{g,e}$ using experimentally determined values of φ. For the case where φ had not been determined at the engine speed selected for the comparisons, a curve of φ against engine speed for the desired coolant-to gas-flow ratio was plotted for the speed range investigated, and the curve was extrapolated to the required engine speed. All blade-temperature-distribution comparisons presented herein have been adjusted to conform to the conditions of blade 8. Blade 8 was used as a basis for comparison because it was the most effectively cooled blade yet investigated.

The comparison of the blade temperatures of the various blade configurations with engine speed was accomplished by the method presented in reference 2.

   Allowable turbine-inlet temperature. - The general method for predicting the allowable turbine-inlet temperature at sea level is discussed in detail in reference 1. Comparison of allowable turbine-inlet temperatures are presented herein for both sea-level and 40,000-foot altitude conditions. The calculation of the 40,000-foot altitude condition was identical with the sea-level calculation except that the values of $T_{g,e}$, $T_{a,e,h}$, and φ had to be predicted at 40,000 feet. The values of $T_{a,e,h}$ were taken as 510° and 200° F at sea level and as 440° F at 40,000 feet. The values of 510° and 440° F were obtained by adding 100° F, the approximate temperature rise of the cooling air from the rotor hub to the blade root, to the compressor discharge temperature computed from NACA standard atmospheric conditions and the compressor-temperature-ratio curves presented in reference 1. The 200° F value was assumed to be the temperature of the cooling air at the blade root

when a heat exchanger is placed between the compressor discharge and the turbine-rotor coolant inlet. The values of φ at a coolant-flow ratio of 0.05 were obtained for the rated engine speed, sea-level conditions by extrapolation of the curves of φ against engine speed. The values of φ for the 40,000-foot altitude condition were obtained by selecting the test data taken at approximately the combustion-gas-flow rate the engine would have at the 40,000-foot altitude with a flight Mach number of 0.8. These data were taken as the 5000 rpm sea-level data.

In order to establish the validity of using the 5000 rpm data for the 40,000-foot altitude condition, the value of φ for 40,000-foot altitude was calculated in the following manner: First, for a particular thermocouple location, curves of φ against w_g for several values of cooling-air flow w_a were plotted. The values of φ used in this plot were obtained by the cross-plot of curves of φ against w_a for the engine speeds (or combustion-gas flows) investigated. Then, the curves of φ against w_g were extrapolated to the combustion-gas flow corresponding to an engine speed of 11,500 rpm at sea-level conditions, thus obtaining a curve of φ against w_a at these conditions. The equation for this last curve was determined by fitting the spanwise-temperature-distribution equation of reference 12 to the curve. The equation, in the notation of the present report, is

$$\varphi = \frac{1}{1 + \lambda} e^{-\frac{1}{1 + \lambda} \frac{H_0 l_0 bx}{c_p w_a b}} - \frac{\omega^2 w_a bx}{gJH_0 l_0 (T_{g,e} - T_{a,e,h}) b} +$$

$$\left(1 - e^{-\frac{1}{1 + \lambda} \frac{H_0 l_0 bx}{c_p w_a b}} \right) \left[\frac{\omega^2 w_a}{gJH_0 l_0} \frac{1}{(T_{g,e} - T_{a,e,h})} \right] \left[\frac{c_p w_a (1 + \lambda)}{H_0 l_0} - r_h \right] \quad (3)$$

where the third term is very small in comparison with the others. Also, as shown in reference 1,

$$\lambda \approx K_1 \frac{w_g^m}{w_a^n} \quad (4)$$

and it can be shown that

$$H_0 l_0 \approx K_2 w_g^m \quad (5)$$

where K_1 and K_2 are constants. Equation (3), neglecting the third term, can be rewritten as

$$\varphi = \frac{1}{1 + K_1 \dfrac{w_g^m}{w_a^n}} e^{\displaystyle -\frac{K_2 w_g^m x}{\left(1 + K_1 \dfrac{w_g^m}{w_a^n}\right) c_p w_a}} - \frac{\omega^2 w_a x}{gJK_2 w_g^m (T_{g,e} - T_{g,e,h})} \tag{6}$$

Now, by choosing two values of w_a and their corresponding values of φ from the curve at an engine speed of 11,500 rpm and sea-level conditions, and assuming that $m = n = 0.8$, the constants K_1 and K_2 can be determined by a trial-and-error method from equation (6). Because the only change in the values employed in equation (6) when going from sea level to altitude is that of w_g and thus w_a, equation (6) was used to calculate φ at 11,500 rpm and 40,000-foot altitude for the desired values of w_a. The results of these calculations were compared with the values of φ obtained from the data at 5000 rpm and sea-level conditions. The maximum deviation of the calculated value of φ from the data value was about 10 percent. Therefore, the use of the 5000 rpm data appears to be justified because these deviations are within the usual scatter of heat-transfer-correlation results.

The results presented in table III were calculated for a design engine speed of 11,500 rpm, a coolant flow equivalent to 5 percent of the combustion-gas flow, and for the nonstrategic Timken alloy 17-22A[S]. As previously indicated, the flight altitudes considered were sea level and 40,000 feet. Flight Mach numbers of 0 and 0.8 were assumed for the sea-level and 40,000-foot altitude conditions, respectively.

Several methods of blade fabrication were considered for calculating the centrifugal stresses in the blade shell. The tubes of blade 8 were assumed to be supported independently of the blade shell. For blade 9, the fins and the tubes were assumed to be supported by the blade shell because it was believed that the relatively high density and low strength of copper would not permit the copper tubes to be self-supporting. Additional stress calculations were made for blade 9 with the assumption that only the large tubes near the leading and trailing edges with copper fins embedded in them (fig. 4) were made of copper; whereas the remaining five tubes were considered to be steel. For this arrangement, the steel tubes were assumed to be independently supported but the copper tubes and fins were supported

by the blade shell. The cooling effectiveness of blade 9 was assumed the same for both the copper and the copper-steel tube arrangement.

The allowable turbine-inlet-temperature calculations were made for two different assumed sets of blade-temperature conditions: (1) The spanwise blade-temperature profile was assumed to be that determined from the extrapolation of the measured φ values along the trailing edge of the blade; (2) the spanwise profile was assumed to have the same shape as that determined by the trailing-edge measurements but was based on extrapolation of the φ values measured at the midchord position. The chordwise gradients were taken as zero for both sets of assumptions.

Cooling-air-pressure loss. - The method of correlating the pressure loss as it passes through the inlet tube and cooling-air passages and into the combustion-gas stream is developed in reference 2. For this loss, the following expression is evaluated:

$$Y = \frac{\rho_{a,H}}{\rho_0} \left[p'_{a,H} - \left(p'_m - \frac{\eta \omega^2 r_T{}^2 \rho_{a,H}}{70.7} \right) \right] \tag{7}$$

where the quantities $\rho_{a,H}$, $p'_{a,H}$, and p'_m are experimentally determined and the compression efficiency η was taken as 0.27. In order to determine the pressure loss through the blades alone, the pressure loss from the rotor hub to the blade root is substracted from equation (7). This loss was evaluated in reference 3.

RESULTS AND DISCUSSION

In all cases, the blade configurations investigated were fabricated without extensive design or aerodynamic studies such as would be required to determine the optimum tube arrangement, slot lengths, and slot locations. The values of cooling effectiveness and pressure loss presented in this report serve to indicate the relative superiority of the special cooling modifications investigated, but improved performance could undoubtedly be obtained by a more thorough design analysis.

The variation of the turbine-inlet-temperature ratio is presented in figure 6 in order to indicate how the turbine-inlet temperatures varied over the speed range investigated.

Observed Blade Temperatures

Comparison of blade and cooling-air temperatures. - The cooling-air-flow distribution to the cooled blades was compared by noting the cooling-air temperatures at the base of each cooled blade. This observation was made at the beginning of the investigation of each blade configuration at an engine speed of 4000 rpm. For each blade configuration, the two cooling-air temperatures at the blade bases agreed very well. It was assumed that because the cooling-air temperatures at the blade bases were the same, the cooling-air-flow rate was also the same. The metal temperatures at similar locations on the cooled blades were also compared and were often found to differ slightly. These differences were attributed to small variations of the coolant-passage geometry between the two blades. Considerable effort was made to fabricate two blades of identical coolant-passage geometry; however, small dimensional variations were unavoidable.

The temperatures of the two modified uncooled blades were also compared at the beginning of each investigation and good agreement was always observed.

Effect of cooling-air flow on blade, effective gas, and cooling-air temperatures. - Figures 7 to 12 present the blade temperatures as they were observed for the highest engine speed at which data were taken during the investigation (most severe conditions of operation) of each blade configuration. In the case of blade 6, a blade failure resulted in the termination of tests at 9000 rpm. For each case, a decrease in cooling-air flow was accompanied by an increase of the cooled-blade temperature for all thermocouple locations. It can be seen that the rate of temperature rise for a decreasing cooling-air flow is greater at the leading edges of blades 6, 7, and 8 than that for the leading edges of blades 4, 5, and 9. At low cooling-air flows, the pressure difference from the coolant passage across the leading-edge slots to the combustion-gas stream would be expected to be less than that across the other cooling-air paths to the combustion-gas stream; therefore, the amount of cooling air flowing through the leading-edge slots was probably a smaller percentage of the total cooling-air flow at the low flow rates than at the high flow rates.

Correlated Cooled-Blade Temperatures

Values of the temperature-difference ratio φ for each of the
cooled-blade thermocouples for the blades investigated are presented
in table II. Data for three engine speeds are given; the minimum, an
intermediate, and the maximum speeds. Values of φ for other speeds
may be interpolated or extrapolated from those given.

Comparison of Blade Temperatures

Chordwise temperature distributions. - The chordwise temperature
profiles, at 35-percent span of the blades investigated, appear in fig-
ure 13. The curves are for an engine speed of 10,000 rpm, a ratio of
cooling-air flow to combustion-gas flow of 0.056, and a cooling-air
temperature at the blade root of 126° F. The curve for blade 8 is from
experimental data. The curves were faired through the limited number
of points available using as a guide more complete temperature-
distribution data (unpublished) obtained in static cascades.

In general, the midchord temperatures of the blades investigated
were approximately one-half that of the effective gas temperature.
Leading-edge temperatures varied from 780° F for blades 7 and 8 to
960° F for blade 5 at an effective gas temperature of 1160° F. At the
same gas temperature, the trailing-edge temperature varied from 740° F
for blade 8 to 1020° F for blade 4. No temperatures were available for
the extreme leading edge of blade 7, but the temperature rise from
location G to the nose was assumed to be less than that for any of the
other blade configurations because of the radial slot exhausting cooling
air directly on the leading edge at the stagnation point. (See fig. 3.)

Blade 9, with the large leading-edge radius and a copper fin to
the leading edge, was cooler at the leading edge than blade 6 with
herringbone slots - 850° F as compared with 900° F. For the
herringbone-slot blade, however, there was no film cooling of a tri-
angular area from the leading edge axially to a slot. (See fig. 2.)

Plugging of the center row of tubes of blade 4 resulted in a
hotter leading-edge temperature than leaving the tubes unplugged -
960° F for blade 5 as compared with 910° F for blade 4. At the mid-
chord, however, the temperature was greatly reduced on the pressure
surface of blade 5 as compared with blade 4. On the suction surface
at the midchord, there was little difference in temperature between
the two blades.

The trailing-edge temperature of blade 8 was about 100° F below that of any of the other configurations investigated. The effect of the supporting strut in the trailing-edge slot at 35-percent span is readily apparent if temperatures of blades 7 and 8 are compared at the trailing edge. The trailing edge of blade 8 was about 170° F lower than that of blade 7. (See fig. 13.) The support effectively separated the cooling air from the trailing-edge surface immediately downstream of the strut, allowing the hot gas to come in contact with the surface of blade 7.

Film cooling of the trailing edge by bleeding cooling air through holes, as shown in figures 1(b) and 2(c), resulted in higher temperatures at the trailing edge than when other devices, such as slots and copper fins, were used in the blades. Plugging the center row of tubes of blade 4, resulting in blade 5, reduced the trailing-edge temperature 25° F, probably because of an increase of coolant through the trailing-edge holes. A similar effect, however, was not observed at the leading edge. Blade 6, with holes twice the diameter of the holes of blade 4, indicated a trailing-edge temperature of 940° F, or about 80° F below that of blade 4. The temperature of blade 4 was taken downstream of a point midway between two hole centers; whereas the temperature of blade 6 was taken at a point downstream of a hole center. Mention has been made of the simple flow investigation conducted on a cascade in which full film coverage of the trailing-edge section was indicated for a configuration as used on blades 4, 5, and 6. Since that time, more refined investigations have been conducted, which indicate that the cooling air streams directly along the blade in a narrow band from the hole rather than spreading uniformly over the trailing-edge section (reference 11).

At the midchord, the blades were cooled equally well except for the pressure surfaces of blade 9. Calculations made of the theoretical effectiveness of blade 9 at the midchord indicated that a poor bond between the copper tubes and the X-40 blade shell must have existed in the experimental blades. The increased conductivity of the copper tubes over the steel tubes of other configurations provided no reduction of the temperature difference between the pressure and suction surfaces of the blade. Better bonding between the copper tubes and the blade shell will probably provide improved cooling effectiveness.

On blades 7 and 8, temperatures were obtained at a point on the pressure surface at 74-percent chord (thermocouple Q, fig. 5(c)). This point is located between the rearmost tube and the trailing-edge slot and the temperature at this point was about equal to that of the leading edge and 40° F higher than that of the trailing edge. This high-temperature point might be eliminated by a redesign of the trailing-edge-section cooling-air passage by using additional tubes and variable slot width.

Effect of increase of cooling air. - The effect of increasing the
cooling-air flow on the chordwise temperature distribution at 35-percent
span of blade 8 is shown in figure 14. A temperature decrease of 120° F
at the midchord, 165° F at the trailing edge, and 180° F at the leading
edge resulted from a doubling of the cooling-air flow. The difference
in temperature between the leading edge and the midchord for both the
pressure and suction surfaces was reduced about 70° F at the higher air
flow, which indicated that a greater percentage of the air was flowing
out the leading-edge slots at the higher air flow.

In order to show the progress of the investigation on cooled
blades, a comparison of the chordwise temperature distributions of the
10-tube blade (reference 1) and the blade that indicated the flattest
temperature distribution of those reported herein, blade 8, is shown
in figure 15. The conditions for the results presented are the same
as those for figure 13. The special modifications of the leading and
trailing edges of blade 8 (fig. 3) resulted in lowering the temperature
of the leading edge, as compared with the 10-tube blade, by 190° F and
that of the trailing edge by 260° F while maintaining midchord temper-
atures at a value approximately one-half that of the effective gas
temperature.

Examination of figure 15 shows that, in general, the maximum dif-
ference of about 450° F between the midchord temperatures and the tem-
perature of the blade extremities for the 10-tube blade has been reduced
to about 230° F for blade 8, a reduction of almost one-half. As was
pointed out in "General Principles of Cooled-Blade Design," the blade
stress patterns in cooled blades containing holes and slots are very com-
plex and cannot be evaluated without simplifying assumptions that seri-
·ously impair the reliability of the results of the analysis. Because of
the uncertainties introduced by the blade stresses, the relative superi-
ority of the different blade designs cannot be stated with reference to
durability in actual engine operation. Radial slots, blade 8, appear
to provide effective cooling; however, the stresses introduced by the
slots may more than overcome the apparent gains achieved by improved
blade cooling. Blades similar to blade 9, which appears to possess
good structual rigidity in addition to good cooling effectiveness,
may provide the best solution to the problem of operating nonstrategic
blades at current inlet gas temperatures. The substitution of steel
tubes for the copper tubes of blade 9 should provide improved cooling
at the midchord position through the elimination of poor bonding
between the blade shell and the tubes. The leading- and trailing-
edge tubes should be copper to insure effective bonding with the
copper fins.

The effect of increasing the leading-edge radius only can be deter-
mined by comparing the results for blade 4 (fig. 13) with the 10-tube
blade (fig. 15). The temperature was reduced from 970° to 910° F. This
reduction is about that which could be obtained theoretically. The
effect on the aerodynamics of the blade, however, may be detrimental at
high Mach numbers, but structual strength and off-design-point perform-
ance may be improved.

Effect of engine speed on blade peripheral temperatures. - Fig-
ure 16 is a plot of blade temperatures around the blade periphery at
35-percent span from the root against engine speed for the blades
reported herein and the 10-tube blade reported in reference 1. The
temperature variations of thermocouples G, H, I, and J are shown in
figures 16(a), 16(b), 16(c), and 16(d), respectively. Standard sea-
level conditions at the compressor inlet and a cooling-air flow to
gas-flow ratio of 0.05 were used in the calculations.

All blade-temperature variations with engine speed followed the
general trend of the curve of effective gas temperature against engine
speed given in reference 2, except for thermocouple J of the 10-tube
blade. A possible explanation of the temperature variation of the
10-tube blade is given in reference 1. The improvement achieved in
cooling the leading and trailing edges through special modifications
over the speed range can be ascertained from figures 16(a) and 16(c)
by comparing the results of blades with these modifications with the
10-tube-blade results. At speeds above 8000 rpm, the leading-edge
temperature of blades 7 and 8 was about 150° F lower than the 10-tube-
blade temperature (fig. 16(a)). In the case of the trailing-edge
temperature, blade 8 became progressively cooler than the other blades
(fig. 16(c)). The trailing-edge temperature of blade 8 averaged about
150° F lower than that of the 10-tube blade above 8000 rpm for the
conditions used in figure 16.

Comparison of Correlated Cooling-Air-Pressure Differences

Plots of the pressure-drop parameter Y calculated from the data
for various cooling-air-flow rates are given in figures 17(a), 17(b),
17(c), 17(d), and 17(e) for blades 4, 5, 7 and 8, 6, and 9, respec-
tively. The parameter Y was determined from equation (7). As pre-
viously mentioned, a value of η of 0.27 was successfully used to
correlate the data of references 2 and 3. Reference to figure 17
shows that the same value of η used to calculate Y for the present
blades also results in good correlation of the present data for all
blades; one curve was applicable for all engine speeds for each
blade.

The faired curves of figure 17 are replotted in figure 18 in order
to obtain a direct comparison of the pressure-drop parameter, and thus
some idea of the cost of cooling each blade. Blades 7 and 8 required
the greatest pressure for forcing the cooling air through the wheel and
the blades; whereas blade 6 required the lowest pressure. Although
blade 9 required a somewhat higher pressure than blade 6, it was con-
siderably more economical to cool than blades 7 and 8.

The foregoing parameter Y discussed in connection with fig-
ures 17 and 18 is a measure of the pressure difference required to
force the coolant from the hub to the blade tip. Figure 19 is a plot
of the pressure parameter Y_1, which is a measure of the pressure
difference from blade root to tip, for all the blades. The order of
the curves as far as pressure required is the same as in figure 18
because the pressure difference required from hub to blade root is
the same for all blades at a given air flow as the same engine type
was used.

The pressure drop required to produce a given cooling effectiveness
is also of interest to the blade designer. For example, the blade-
pressure loss required to obtain a trailing-edge cooling effectiveness
of 0.2 at 10,000 rpm for the configurations investigated would be
approximately as follows: Blade 4, 90 inches of mercury; blade 5,
100 inches of mercury; blade 6, 4 inches of mercury; blade 7, 20 inches
of mercury; blade 8, 10 inches of mercury; and blade 9, 1 inch of
mercury. This comparison may be changed somewhat if other values of
required cooling effectiveness and blade position are selected. For
these conditions, however, blade 9 apparently affords the best com-
bination of pressure loss and trailing-edge cooling of any of the
configurations investigated.

The pressure loss must be small enough that the compressor-
discharge pressure will be adequate to provide the required cooling-
air-flow rate. If an axial-flow compressor is used, the cycle perform-
ance can be improved by appropriate interstage bleedoffs so as to
minimize the compressor work done on the cooling air.

Predicted Allowable Turbine-Inlet Temperatures

NACA standard sea-level conditions. - A summary of the results
of the allowable turbine-inlet temperatures for the conditions for which
the predictions were made is shown in table III for blades 8 and 9 and
a configuration similar to blade 9 but having five steel tubes in the
midchord region of the blades while retaining the two copper tubes to
which the copper fins were attached. For sea-level conditions, cooling

air bled directly from the compressor $(T_{a,e,h} = 510^{\circ}$ F), and calcu-
lations based on the trailing-edge temperatures, blade 8 would permit a
turbine-inlet temperature of 1520° F; whereas blade 9 with all copper
tubes and with a copper-steel tube arrangement would permit turbine-
inlet temperatures of 1490° F and 1520° F, respectively. By employing
an intercooler, which would reduce the cooling-air temperature at the
blade root to 200° F, the allowable turbine-inlet temperature could be
increased about 160° F for both blades 8 and 9 with all copper tubes.

When the allowable turbine-inlet temperature is calculated on the
basis that the entire blade cools as well as the midchord position, the
allowable temperature for blade 8 was increased from 1520° F to 2040° F,
an increase of 520° F. For blade 9, the increase was about 300° F for
both the all-copper, and the copper-steel tube arrangement. By
employing an intercooler and having a cooling-air temperature of 200° F,
the turbine-inlet temperature could be increased 440° F for blade 8 and
350° F for blade 9 with all copper tubes.

Altitude of 40,000 feet. - At an altitude of 40,000 feet, the
allowable turbine-inlet temperature for blade 8, when based on the
trailing-edge temperatures with the cooling air bled directly from the
compressor $(T_{a,e,h} = 440^{\circ}$ F), is 1460° F, a decrease of 60° F from
that permitted at sea-level. For the same conditions, the allowable
temperature for blade 9 with all copper tubes was 1530° F, an increase
of 40° above that allowed at sea-level. These variations are of the
same magnitude as the variations introduced by the uncertainties of
the method of determining the values of φ at the altitude condition.
Apparently the variation of allowable turbine-inlet temperature between
sea level and 40,000 feet is small because the decrease in cooling-air
inlet temperature balances the increase of the over-all heat-transfer
coefficient between the combustion gas and the cooling air.

When the allowable turbine-inlet temperature is based on the
midchord temperatures (table III), blade 8 could be operated at an
inlet temperature of 1890° F and blade 9 could be operated at an inlet
temperature of 1760° F. On the midchord basis, the same trend observed
at sea level is apparent; that is, blade 8 could be operated at higher
inlet temperature than blade 9 because the midchord temperatures of
blade 8 are about 50° F less than those of blade 9.

Of the blade configurations investigated, blades 8 and 9 show the
most promise of permitting operation of the turbine at current turbine-
inlet temperatures when the blades are made of nonstrategic materials.
It is shown in table III that these blades can be operated at turbine-
inlet temperatures of 1500° F even when the calculations are based on
the temperature of the trailing edge, which is the hottest portion of

the blade. It should be emphasized that these predicted turbine-inlet temperatures were based on consideration of only the simple centrifugal stresses in the cooled blade; vibratory and thermal stresses were neglected. Because of the thermal gradients present in the blades, a transfer of stress from the hot leading edges to the cooler midchord portion will probably occur. If the vibratory stresses, which were neglected in these calculations, are not significant, then the actual limiting turbine-inlet temperature will be between the limiting value based on the midchord temperatures and the values based on the trailing-edge temperatures.

SUMMARY OF RESULTS

The results of this experimental investigation of several air-cooled turbine blades with special modifications for cooling the leading and trailing edges of the blades are as follows:

1. The chordwise thermal gradients were reduced as compared with blades having no special leading- and trailing-edge modifications.

2. Of the leading-edge modifications investigated, the order of increasing cooling effectiveness was (1) the increased leading-edge radius (blades 4 and 5), (2) the herringbone slots (blade 6), (3) the combination of increased leading-edge radius and copper fin (blade 9), and (4) the combination of increased leading-edge radius and radial slots (blades 7 and 8).

3. Of the trailing-edge modifications investigated, the order of increasing cooling effectiveness was (1) radial groove in the pressure surface fed by 0.020-inch diameter holes (blade 4), (2) radial groove in the pressure surface fed by 0.040-inch-diameter holes (blades 5 and 6), (3) copper fin (blade 9), and (4) radial slots (blades 7 and 8).

4. The plugging of the central cooling-air passages (blade 5) resulted in a higher leading-edge temperature but gave increased cooling at the midchord and trailing-edge sections.

5. At an engine speed of 10,000 rpm, an effective gas temperature of 1160° F, and a coolant- to combustion-gas-flow ratio of 0.056, the most effectively cooled blade (blade 8) had a maximum chordwise temperature variation of about 230° F as compared with 450° F for a blade with no special provision for cooling the leading and trailing edges of the blades.

6. At these same engine conditions, the leading-edge, average midchord, and trailing-edge temperatures for the most effectively cooled blade were about 780°, 590°, and 740° F, respectively.

7. Blades 7 and 8 required the greatest pressure to force a given quantity of cooling air through the blades; blade 6 required the least. Blade 9 exhibited a promising combination of structural strength, good cooling effectiveness, and low cooling-air-pressure loss.

8. The allowable turbine-inlet temperature predicted by the methods utilized (which assumed uniform distribution of the simple centrifugal stresses and neglected thermal and vibratory stresses) indicated that blades 8 and 9, when fabricated of nonstrategic materials, might be operated at current turbine-inlet temperatures.

Lewis Flight Propulsion Laboratory,
    National Advisory Committee for Aeronautics,
        Cleveland, Ohio.

APPENDIX - SYMBOLS

The following symbols are used in this report:

b blade span, ft

c_p specific heat at constant pressure of cooling air, Btu/(lb)($^\circ$F)

g acceleration due to gravity, 32.2 ft/sec^2

H average heat-transfer coefficient, Btu/(sq ft)($^\circ$F)(sec)

J mechanical equivalent of heat, 778 ft-lb/Btu

K_1, K_2 constants of equation (6)

l perimeter of cooled blade, ft

m exponent

N engine speed, rpm

n exponent

p' total pressure, in. Hg

R ratio of coolant flow per blade to combustion-gas flow per blade, coolant-flow ratio

r radius from center of rotor, ft

T static temperature, $^\circ$F

w weight-flow rate, lb/sec

w_F fuel flow, lb/hr

x leading-edge radius, ft

Y pressure-drop parameter, from rotor hub to blade tip,

$$\frac{\rho_{a,H}}{\rho_0}\left[p'_{a,H} - \left(p'_m - \frac{\eta \omega^2 r_T^2 \rho_{a,H}}{70.7} \right) \right], \text{ in. Hg}$$

Y_1 pressure-drop parameter, from blade root to tip,

$$\frac{\rho_{a,H}}{\rho_0}\left[p'_{a,H} - \left(p'_m - \frac{\eta\omega^2 r_T^2 \rho_{a,H}}{70.7}\right)\right] - (p_{a,H} - p_{a,e,h})$$

η efficiency of compression in turbine wheel

λ $H_o l_o / H_f l_i$

ρ density, slugs/cu ft

φ temperature-difference ratio, $(T_{g,e} - T_B)/(T_{g,e} - T_{a,e,h})$

ω angular velocity of rotor, radians/sec

Subscripts:

A   combustion air

a   blade-cooling air

B   cooled blade

c   compressor

e   effective

f   blade wall to cooling air

g   combustion gas

H   hub of rotor

h   root of blade

i   inlet or inside of cooled-blade wall

m   mixture of combustion gas and scavenge, bearing, and blade-
       cooling air in tail pipe

O   NACA standard sea-level conditions

o   outlet or outside wall of cooled blade
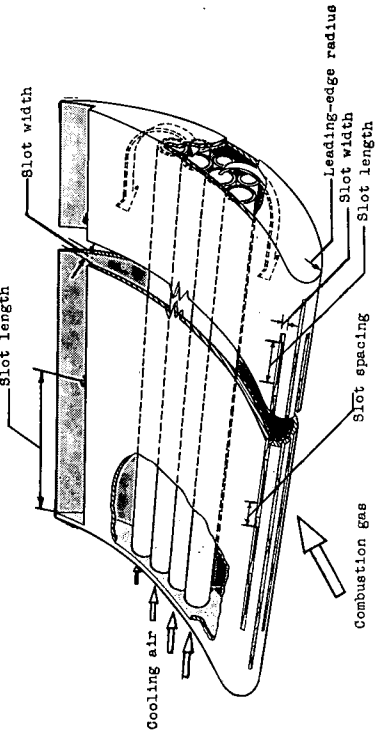
S   stator

T   blade tip

REFERENCES

1. Ellerbrock, Herman H., Jr., and Stepka, Francis S.: Experimental
     Investigation of Air-Cooled Turbine Blades in Turbojet Engine.
     I - Rotor Blades with 10 Tubes in Cooling-Air Passages. NACA
     RM E50I04, 1950.

2. Hickel, Robert O., and Ellerbrock, Herman H., Jr.: Experimental
     Investigation of Air-Cooled Turbine Blades in Turbojet Engine.
     II - Rotor Blades with 15 Fins in Cooling-Air Passages. NACA
     RM E50I14, 1950.

3. Hickel, Robert O., and Smith, Gordon T.: Experimental Investiga-
     tion of Air-Cooled Turbine Blades in Turbojet Engine. III -
     Rotor Blades with 34 Steel Tubes in Cooling-Air Passages. NACA
     RM E50J06, 1950.

4. Dempsey, W. W.: Turbine Blade Cooling (Final Hot Test Rep.). Rep.
     No. 2037, Stalker Development Co., June 29, 1949.

5. Kuepper, K. H.: Temperature Measurement on Two Stationary Bucket
     Profiles for Gas Turbines with Boundary-Layer Cooling. Trans.
     No. F-TS-1543-RE, Air Materiel Command, U.S. Air Force, Jan.
     1948. (ATI No. 18576, CADO.)

6. Vincent, E. T.: The Theory and Design of Gas Turbines and Jet
     Engines. McGraw-Hill Book Co., Inc., 1950, pp. 482-495.

7. Kearton, William J.: Steam Turbine Theory and Practice. Pitman
     Pub. Corp., 5th ed., 1948, pp. 302-313.

8. Pollman, Erich: Temperatures and Stresses on Hollow Blades for
     Gas Turbines. NACA TM 1183, 1947.

9. Boelter, L. M. K., Cherry, V. H., Johnson, H. A., and Martinelli,
     R. C.: Heat Transfer Notes. Univ. Calif. Press (Berkeley), 1948.

10. Eckert, E. R. G.: Introduction to the Transfer of Heat and Mass.
     McGraw-Hill Book Co., Inc., 1950.

11. Eckert, E. R. G., Jackson, Thomas W., and Francisco, Allen C.:
     Investigations of Slot Configurations for Film-Cooled Turbine
     Blades by Flow Vizualization Methods. NACA RM E50K01, 1950.

12. Livingood, John N. B., and Brown, W. Byron: Analysis of Spanwise
     Temperature Distribution in Three Types of Air-Cooled Turbine
     Blades. NACA Rep. 994, 1950.

TABLE I – SUMMARY OF GEOMETRY FACTORS AND MODIFICATIONS FOR BLADES INVESTIGATED

Item	Blade 4	Blade 5	Blade 6	Blade 7	Blade 8	Blade 9
Total free-flow area of internal cooling-air passages, sq in.	0.12	0.10	0.17	0.08	0.08	0.17
Total surface area of internal cooling-air passages, sq in.	27.4	21.6	27.0	11.6	11.6	26.5
Total perimeter of internal cooling-air passages, in.	6.8	5.4	6.7	2.9	2.9	6.5
Hydraulic diameter of internal cooling-air passages, in.	0.07	0.07	0.10	0.12	0.12	0.10
Leading-edge modifications	(1) Rounded leading edge Leading-edge radius, 0.099 inch	(1) Rounded leading edge Leading-edge radius, 0.099 inch	(1) Herringbone slots[1] Length of slots, 0.25 inch Width of slots, 0.0105 inch Number of slots, 14 Spacing of slots, 0.25 inch Total free-flow area, 0.037 square inch Sharp leading edge (radius 0.05 inch)	(1) Rounded leading edge Leading-edge radius, 0.099 inch (2) Radial leading-edge slots[2] Length of slots, 0.375 inch Width of slots, 0.010 inch Number of slots, 16 Spacing of slots, 0.1875 inch Total free-flow area, 0.060 square inch	(1) Rounded leading edge Leading-edge radius, 0.099 inch (2) Radial leading-edge slots[2] Length of slots, 0.375 inch Width of slots, 0.010 inch Number of slots, 16 Spacing of slots, 0.1875 inch Total free-flow area, 0.060 square inch	(1) Rounded leading edge Leading-edge radius, 0.099 inch (2) Copper fin extending from inside surface, of leading edge to first internal tube.[3]
Trailing-edge modifications	(1) Radial groove fed by holes Diameter of holes, 0.02 inch Number of holes, 28 Spacing of holes, 0.125 inch Total free-flow area of holes, 0.099 square inch Depth of groove, 0.015 inch Length of groove, 3.975 inches	(1) Radial groove fed by holes[1] Diameter of holes, 0.04 inch Number of holes, 28 Spacing of holes, 0.125 inch Total free-flow area of holes, 0.035 square inch Depth of groove, 0.015 inch Length of groove, 3.975 inches		(1) Radial slots[2] Length of slot, 0.875 inch Width of slot, 0.025 inch Number of slots, 3 Total free-flow area of slots, 0.066 square inch	(1) Radial slots[2] Length of slot, 3.125 inches Width of slot, 0.025 inch Number of slots, 1 Total free-flow area of slots, 0.078 square inch	(1) Trailing edge containing embedded copper fin extending to rear internal tube.

[1] See figure 2.
[2] See figure 3.
[3] See figure 4.

Cooling air

Combustion gas

Slot length

Slot spacing

Slot length

Slot width

Leading-edge radius

Slot width

Slot length

NACA

TABLE II - SUMMARY OF ENGINE OPERATING CONDITIONS AND TEMPERATURE-DIFFERENCE RATIOS

(a) Blade 4

Series	Engine speed N (rpm)	Fuel flow w_F (lb/hr)	Average conditions at compressor inlet		Cooling-air flow per blade w_a (lb/sec)	Coolant flow per blade / Combustion-gas flow per blade R	Temperature-difference ratio φ			
			Total pressure $p'_{A,c,1}$ (in. Hg)	Total temperature $T'_{A,c,1}$ (°F)			Thermocouple			
							G	J	C	H
1	4003	1070	29.18	57	0.103	0.268	0.539	0.816	0.342	0.753
	4001				.089	.231	.516	.801	.339	.729
	3996				.075	.196	.492	.783	.329	.708
	4001				.060	.157	.454	.758	.315	.679
	4005				.050	.131	.427	.733	.308	.658
	4001				.040	.104	.397	.710	.298	.632
	4001				.030	.079	.351	.664	.278	.583
	4001				.020	.052	.299	.605	.257	.530
	4005				.010	.026	.242	.527	.225	.467
2	6000	1475	29.16	82	0.122	0.210	0.509	0.738	0.325	0.746
	6000				.098	.168	.473	.737	.313	.714
	6000				.070	.122	.418	.696	.292	.679
	6000				.048	.084	.371	.660	.273	.642
	6000				.040	.068	.291	.582	.239	.578
	6000				.030	.051	.256	.548	.214	.518
	6000				.020	.035	.238	.524	.206	.500
	6000				.015	.026	.209	.479	.188	.450
	6000				.010	.017	.195	.460	.178	.430
3	9020	2330	29.46	59	0.122	0.127	0.464	0.697	0.229	0.587
	8990				.098	.102	.428	.663	.215	.545
	9020				.070	.072	.377	.631	.194	.484
	9000				.050	.052	.326	.591	.170	.432
	9000				.039	.040	.307	.569	.162	.409
	8990				.030	.031	.275	.540	.147	.382
	9000				.020	.021	.243	.507	.126	.352
	9010				.015	.016	.236	.481	.113	.327
	8990				.010	.010	.199	.445	.064	.280
							A	D	C	P
1	3999	1065	29.13	60	0.103	0.266	0.231	0.459	0.346	0.425
	4001				.090	.232	.232	.452	.340	.406
	3996				.075	.193	.229	.444	.331	.378
	3996				.060	.155	.233	.431	.320	.349
	4001				.050	.129	.230	.421	.314	.324
	3999				.040	.103	.224	.408	.299	.297
	4001				.030	.077	.212	.392	.281	.263
	3999				.020	.051	.188	.365	.252	.221
	4001				.010	.026	.155	.330	.218	.173
2	5990	1455	29.13	85	0.121	0.211	0.205	0.406	0.320	0.413
	6000				.097	.169	.199	.387	.302	.371
	6010				.069	.121	.217	.375	.290	.331
	6000				.048	.084	.214	.356	.272	.288
	6000				.040	.070	.205	.340	.253	.260
	6010				.030	.053	.195	.323	.235	.234
	6000				.020	.035	.174	.299	.210	.197
	6000				.014	.024	.164	.292	.201	.182
	6000				.010	.017	.143	.272	.183	.161
3	9000	2290	29.20	75	0.122	0.131	(a)	0.352	0.245	0.349
	9010				.098	.105		.336	.230	.327
	9010				.070	.075		.312	.212	.272
	9010				.049	.052		.290	.186	.226
	9020				.040	.043		.275	.173	.207
	9010				.030	.032		.261	.161	.187
	9010				.020	.021		.246	.144	.184
	9020				.015	.016		.232	.131	.149
	9010				.008	.009		.208	.104	.134

(a) No data taken.

TABLE II - SUMMARY OF ENGINE OPERATING CONDITIONS AND TEMPERATURE-DIFFERENCE RATIOS - Continued

(b) Blade 5

Series	Engine speed N (rpm)	Fuel flow w_F (lb/hr)	Total pressure $P'_{A,c,i}$ (in. Hg)	Total temperature $T'_{A,c,i}$ (°F)	Cooling-air flow per blade w_a (lb/sec)	Coolant flow per blade / Combustion-gas flow per blade R	Temperature-difference ratio φ			
							Thermocouple			
							G	J	I	H
4	3,998	1020	29.15	71	0.122	0.327	0.579	0.837	0.369	0.793
	4,000				.098	.262	.533	.807	.330	.755
	4,000				.070	.188	.477	.764	.315	.710
	4,000				.049	.131	.424	.710	.295	.654
	3,998				.040	.107	.398	.678	.287	.624
	4,000				.030	.080	.361	.630	.276	.582
	4,000				.020	.054	.296	.547	.256	.509
	4,005				.015	.040	.264	.499	.242	.466
	4,000				.010	.027	.236	.462	.225	.432
5	5,996	1440	29.15	72	0.122	0.206	0.519	0.774	0.306	0.724
	6,000				.098	.165	.476	.744	.290	.694
	5,998				.070	.118	.424	.697	.275	.642
	5,998				.049	.082	.373	.639	.261	.587
	6,000				.040	.068	.345	.604	.250	.556
	6,003				.030	.051	.306	.554	.225	.511
	6,017				.020	.034	.263	.500	.217	.457
	6,000				.015	.025	.243	.468	.204	.430
	6,025				.010	.017	.187	.379	.157	.346
6	10,027	2820	29.17	75	0.121	0.112	0.426	0.699	0.206	0.630
	10,015				.098	.091	.386	.671	.196	.588
	10,020				.070	.065	.336	.615	.180	.531
	10,015				.049	.045	.294	.562	.166	.478
	10,025				.040	.037	.275	.529	.155	.451
	10,031				.035	.032	.255	.513	.145	.436
	10,025				.020	.019	.244	.491	.138	.428
	10,003				.014	.013	.215	.449	.128	.376
	9,996				.010	.009	.181	.400	.095	.320
							A	C	D	P
4	3,993	1020	29.11	70	0.122	0.321	0.240	0.591	0.367	0.441
	3,995				.098	.258	.233	.578	.358	.416
	3,998				.070	.184	.233	.563	.333	.369
	3,995				.049	.128	.228	.541	.318	.329
	3,998				.040	.106	.218	.528	.308	.305
	3,998				.030	.080	.212	.510	.293	.268
	3,995				.020	.052	.194	.490	.268	.226
	4,003				.015	.037	.178	.475	.254	.206
	3,995				.010	.026	.160	.465	.233	.183
5	6,003	1450	29.11	66	0.122	0.206	0.219	0.521	0.328	0.383
	6,000				.098	.165	.230	.501	.313	.358
	6,012				.070	.118	.233	.482	.297	.310
	6,008				.050	.084	.223	.462	.280	.269
	6,005				.040	.067	.209	.442	.261	.241
	6,008				.030	.050	.194	.432	.247	.216
	6,008				.024	.040	.188	.424	.233	.198
	6,014				.015	.025	.168	.404	.209	.166
	6,012				.010	.017	.157	.396	.197	.152
6	9,998	2825	29.16	68	0.123	0.112	0.292	0.420	0.214	0.280
	10,000				.098	.089	.283	.412	.206	.256
	9,996				.070	.064	.251	.381	.184	.210
	10,000				.049	.045	.231	.361	.166	.173
	9,991				.040	.036	.217	.352	.155	.155
	9,998				.030	.028	.196	.335	.135	.133
	10,013				.020	.018	.184	.329	.125	.118
	10,005				.014	.013	.170	.319	.110	.098
	10,003				.010	.009	.163	.307	.101	.090

TABLE II - SUMMARY OF ENGINE OPERATING CONDITIONS AND TEMPERATURE-DIFFERENCE RATIOS - Continued

(c) Blade 6

Series	Engine speed N (rpm)	Fuel flow w_F (lb/hr)	Total pressure $P'_{A,c,i}$ (in. Hg)	Total temperature $T'_{A,c,i}$ (°F)	Cooling-air flow per blade w_a (lb/sec)	Coolant flow per blade / Combustion-gas flow per blade R	G	H	I	J
	4007				0.098	0.265	0.650	0.745	0.396	0.734
	3985				.070	.189	.600	.700	.382	.693
	4017				.049	.132	.528	.648	.355	.654
	3991				.040	.108	.489	.620	.340	.627
7	3993	1055	29.32	80	.030	.081	.448	.578	.315	.593
	3987				.024	.065	.419	.558	.298	.571
	3987				.019	.057	.404	.536	.287	.560
	3985				.015	.041	.370	.508	.265	.540
	3989				.010	.027	.302	.466	.217	.506
	6003				0.098	0.168	0.583	0.680	0.365	0.679
	6000				.070	.120	.523	.634	.344	.644
	5996				.059	.101	.482	.609	.331	.619
	5998				.049	.084	.442	.588	.313	.604
8	6000	1430	29.08	82	.041	.070	.428	.560	.293	.584
	6003				.031	.053	.394	.536	.256	.559
	6000				.024	.040	.371	.510	.246	.547
	6005				.019	.032	.347	.492	.229	.529
	6000				.015	.026	.284	.447	.170	.501
	9013				0.120	0.129	(a)	0.620	0.325	0.648
	9003				.097	.104		.589	.308	.625
	9005				.088	.094		.575	.296	.618
	8991				.069	.074		.547	.274	.592
9	9001	2230	29.41	94	.059	.063		.540	.259	.578
	8998				.049	.053		.506	.238	.568
	8998				.040	.043		.494	.229	.547
	9003				.035	.037		.486	.218	.542
	9003				.030	.032		.466	.197	.531

Series	Engine speed N (rpm)	Fuel flow w_F (lb/hr)	Total pressure $P'_{A,c,i}$ (in. Hg)	Total temperature $T'_{A,c,i}$ (°F)	Cooling-air flow per blade w_a (lb/sec)	Coolant flow per blade / Combustion-gas flow per blade R	A	C	D	P
	4000				0.098	0.258	0.335	0.426	0.497	0.643
	3989				.070	.184	.311	.409	.458	.581
	3993				.050	.131	.294	.383	.429	.504
	3991				.040	.105	.283	.367	.415	.448
7	3985	1060	29.34	70	.030	.079	.277	.339	.389	.363
	3991				.024	.063	.268	.325	.375	.330
	3995				.020	.053	.259	.311	.362	.295
	4010				.015	.039	.248	.290	.344	.247
	4005				.010	.026	.218	.261	.328	.144
	5991				0.098	0.167	0.332	0.399	0.433	0.556
	6003				.070	.119	.312	.372	.396	.476
	6000				.049	.083	.302	.334	.359	.374
	6005				.040	.068	.290	.315	.347	.335
8	6000	1440	29.08	80	.030	.051	.268	.286	.326	.286
	6000				.024	.041	.253	.269	.318	.250
	5998				.020	.034	.233	.256	.306	.202
	6000				.015	.025	.205	.228	.291	.095
	6000									
	9015				0.121	0.130	0.375	0.364	0.376	0.466
	8993				.097	.104	.374	.342	.360	.417
	9010				.088	.095	.372	.334	.348	.392
	9003				.069	.074	.360	.312	.330	.320
9	8996	2210	29.41	92	.058	.062	.346	.292	.317	.288
	9001				.049	.052	.326	.276	.302	.248
	9001				.040	.043	.307	.261	.290	.211
	9003				.030	.032	.280	.234	.279	.091

(a) No data taken.

TABLE II - SUMMARY OF ENGINE OPERATING CONDITIONS AND TEMPERATURE-DIFFERENCE RATIOS - Continued

(d) Blade 7

Series	Engine speed N (rpm)	Fuel flow w_F (lb/hr)	Average conditions at compressor inlet		Cooling-air flow per blade w_a (lb/sec)	Coolant flow per blade / Combustion-gas flow per blade R	Temperature-difference ratio φ			
			Total pressure $p'_{A,c,i}$ (in. Hg)	Total temperature $T'_{A,c,i}$ (°F)			Thermocouple			
							G	H	I	J
10	4003	1075	29.21	90	0.088	0.246	0.576	0.726	0.484	0.764
	3998				.069	.193	.546	.697	.458	.733
	4000				.049	.137	.511	.651	.412	.685
	4000				.040	.111	.487	.620	.385	.656
	3995				.030	.083	.445	.576	.344	.612
	3998				.019	.053	.373	.505	.293	.533
	4000				.015	.042	.289	.452	.252	.468
	4000				.010	.028	.198	.382	.208	.391
	4000				.005	.014	.102	.299	.159	.297
11	6003	1515	29.08	92	0.088	0.156	0.600	0.666	0.417	0.723
	5998				.069	.122	.562	.635	.386	.690
	6000				.049	.086	.500	.581	.340	.632
	6000				.040	.071	.455	.548	.312	.608
	6003				.030	.053	.381	.505	.274	.540
	6000				.019	.033	.246	.429	.222	.444
	6000				.015	.026	.179	.380	.193	.387
	6003				.010	.018	.102	.331	.167	.327
	6000				.008	.014	.084	.307	.153	.303
12	9003	2400	29.22	87	0.103	0.110	0.614	0.608	0.373	0.699
	8993				.089	.095	.591	.585	.358	.678
	8993				.070	.074	.540	.545	.324	.639
	8991				.059	.063	.493	.515	.299	.607
	9001				.049	.052	.423	.481	.271	.567
	8993				.040	.043	.332	.442	.238	.520
	8989				.035	.037	.292	.425	.225	.489
	9001				.030	.032	.228	.394	.209	.451
	8989				.025	.027	.155	.366	.192	.414
							A	C	D	P
10	3998	1075	29.13	84	0.089	0.249	0.670	0.473	0.573	0.621
	4003				.069	.163	.633	.442	.541	.587
	4000				.049	.137	.578	.397	.496	.533
	4003				.040	.111	.543	.364	.468	.500
	4000				.030	.083	.504	.331	.428	.451
	4003				.019	.052	.433	.272	.378	.378
	3998				.015	.028	.392	.239	.353	.333
	4003				.008	.022	.310	.172	.304	.253
	3995				.005	.014	.269	.142	.283	.214
11	5998	1525	29.20	93	0.088	0.154	0.614	0.402	0.508	0.546
	5996				.069	.121	.579	.398	.475	.508
	6000				.049	.086	.522	.326	.422	.448
	6003				.040	.070	.493	.306	.399	.419
	6000				.030	.053	.445	.263	.360	.370
	6000				.020	.035	.383	.208	.317	.301
	6003				.015	.026	.346	.180	.296	.266
	5993				.010	.018	.302	.151	.271	.228
	6000				.008	.014	.283	.139	.266	.215
12	8993	2404	29.18	89	0.102	0.109	0.560	0.381	0.449	0.479
	9005				.088	.094	.553	.354	.420	.447
	9003				.069	.074	.520	.316	.388	.409
	8991				.059	.063	.494	.292	.355	.377
	8991				.049	.052	.473	.262	.341	.347
	8998				.040	.043	.441	.235	.313	.316
	8991				.035	.037	.423	.217	.293	.293
	9003				.030	.032	.398	.196	.274	.272
	8996				.025	.027	.375	.177	.260	.248

TABLE II - SUMMARY OF ENGINE OPERATING CONDITIONS AND TEMPERATURE-DIFFERENCE RATIOS - Continued

(e) Blade 8

Series	Engine speed N (rpm)	Fuel flow w_F (lb/hr)	Total pressure $P'_{A,c,i}$ (in. Hg)	Total temperature $T'_{A,c,i}$ (°F)	Cooling-air flow per blade w_a (lb/sec)	Coolant flow per blade / Combustion-gas flow per blade R	Temperature-difference ratio φ Thermocouple			
							G	C	H	J
13	(a)	(a)	(a)	(a)	(a)	(a)	(a)	(a)	(a)	(a)
14	(a)	(a)	(a)	(a)	(a)	(a)	(a)	(a)	(a)	(a)
15	9,989	3080	29.16	87	0.117	0.110	0.580	0.570	0.595	0.709
	9,996				.098	.092	.556	.526	.572	.678
	10,000				.070	.066	.469	.446	.513	.619
	10,000				.060	.056	.412	.408	.482	.588
	9,996				.055	.052	.387	.387	.465	.576
	10,005				.049	.046	.334	.363	.444	.548
	9,989				.044	.041	.297	.340	.428	.530
	10,000				.040	.038	.264	.319	.409	.511
							A	C	D	Q
13	4,005	980	29.13	85	0.088	0.240	0.640	0.690	0.564	0.638
	3,989				.069	.189	.606	.645	.535	.604
	3,998				.049	.134	.554	.574	.492	.551
	3,995				.040	.110	.538	.531	.467	.518
	3,995				.030	.082	.484	.460	.429	.467
	3,998				.019	.052	.419	.363	.381	.391
	3,991				.015	.041	.384	.306	.354	.352
	3,989				.010	.027	.333	.236	.320	.293
	3,987				.008	.022	.306	.204	.301	.264
14	5,998	1510	29.13	88	0.089	0.154	0.603	0.631	0.503	0.569
	6,010				.070	.121	.570	.582	.472	.530
	6,012				.049	.085	.520	.498	.420	.467
	6,010				.040	.069	.494	.452	.396	.438
	6,003				.030	.052	.451	.380	.360	.386
	6,012				.024	.042	.421	.336	.342	.353
	6,008				.019	.033	.390	.288	.315	.315
	6,008				.015	.026	.358	.238	.293	.279
	6,012				.010	.017	.316	.188	.267	.238
15	10,008	3030	29.14	89	0.116	0.110	0.587	0.378	0.458	0.485
	10,003				.098	.093	.571	.349	.438	.456
	9,993				.079	.075	.540	.314	.403	.418
	9,996				.070	.066	.521	.295	.385	.394
	10,000				.059	.056	.499	.270	.362	.365
	9,996				.049	.047	.475	.244	.335	.334
	9,993				.044	.042	.457	.229	.317	.318
	9,993				.040	.038	.442	.219	.308	.303

(a) No data taken.

TABLE II - SUMMARY OF ENGINE OPERATING CONDITIONS AND TEMPERATURE-DIFFERENCE RATIOS - Concluded

(f) Blade 9

Series	Engine speed N (rpm)	Fuel flow w_F (lb/hr)	Total pressure $p'_{A,c,i}$ (in. Hg)	Total temperature $T'_{A,c,i}$ (°F)	Cooling-air flow per blade w_a (lb/sec)	Coolant flow per blade / Combustion-gas flow per blade R	G	H	J	P
16	4,000 3,998 4,003 4,000 3,995 3,995 4,000 4,000 4,000	1018	29.32	72	0.089 .070 .049 .040 .030 .020 .015 .010 .008	0.232 .182 .126 .103 .077 .051 .038 .026 .021	0.568 .539 .502 .470 .423 .368 .327 .293 .269	0.678 .644 .592 .561 .510 .452 .414 .373 .345	0.731 .696 .643 .608 .557 .490 .453 .408 .380	0.465 .445 .411 .392 .350 .303 .271 .237 .219
17	7,012 7,005 6,996 7,005 7,003 6,993 7,020 7,003 6,986	1880	29.28	72	0.099 .080 .059 .049 .040 .036 .030 .024 .020	0.135 .109 .081 .067 .055 .049 .041 .033 .027	0.523 .496 .455 .421 .393 .377 .356 .335 .315	0.582 .547 .504 .476 .444 .432 .408 .395 .372	0.656 .623 .579 .540 .512 .498 .468 .455 .430	0.409 .384 .349 .322 .300 .289 .272 .255 .238
18	10,008 9,991 9,996 9,996 9,989 10,003 9,998 9,996	2950	29.17	96	0.122 .097 .079 .059 .049 .040 .030 .021	0.114 .090 .073 .055 .045 .037 .028 .019	0.482 .445 .419 .373 .345 .321 .291 .266	0.547 .512 .484 .440 .417 .395 .369 .339	0.644 .603 .572 .524 .494 .469 .435 .404	0.391 .363 .331 .291 .274 .255 .230 .207
							A	C	D	R
16	3,998 4,000 4,000 3,995 4,000 3,998 3,995 4,000 3,998	1125	29.32	72	0.104 .070 .049 .040 .030 .020 .015 .010 .008	0.269 .180 .126 .102 .077 .051 .038 .026 .020	0.515 .492 .463 .446 .413 .375 .351 .317 .293	0.561 .530 .491 .469 .431 .383 .353 .328 .303	0.630 .600 .570 .554 .522 .481 .457 .436 .415	0.743 .707 .654 .622 .572 .504 .465 .422 .389
17	7,012 7,000 6,993 7,000 7,008 7,015 7,015 6,996 7,010	1810	29.29	74	0.099 .080 .060 .049 .040 .024 .020 .015 .010	0.135 .109 .082 .067 .055 .033 .028 .021 .014	0.458 .440 .403 .383 .363 .320 .301 .278 .245	0.454 .438 .403 .380 .364 .317 .301 .283 .255	0.519 .502 .472 .458 .438 .399 .387 .373 .350	0.660 .633 .581 .551 .520 .459 .435 .405 .362
18	10,000 9,993 10,008 10,005 9,989 10,000 10,008 10,000	2940	29.16	93	0.122 .098 .079 .059 .049 .040 .030 .021	0.113 .091 .073 .054 .045 .037 .029 .019	0.431 .416 .400 .376 .356 .338 .318 .296	0.401 .376 .351 .320 .304 .289 .273 .252	0.489 .462 .439 .411 .398 .385 .373 .356	0.657 .619 .585 .539 .512 .485 .454 .416

TABLE III - PREDICTED ALLOWABLE TURBINE-INLET TEMPERATURES FOR TIMKEN ALLOY 17-22A[S]

[Engine speed, 11,500 rpm; cooling-air-flow rate, 5 percent of combustion-gas-flow rate; atmospheric conditions at compressor inlet, standard sea level and 40,000 feet, flight Mach number of 0.8 at altitude]

Blade	Cooling-air inlet temperature $T_{a,e,h}$ (°F)	Allowable turbine-inlet temperatures, °F			
		Based on trailing-edge temperatures		Based on midchord temperatures	
		Sea level	40,000 feet	Sea level	40,000 feet
8	510	1520		2040	
	a200	1680		2480	
	440		1460		1890
9 having seven copper-tube inserts	510	1490		1800	
	a200	1650		2150	
	440		1530		1760
9 having five steel- and two copper- tube inserts	510	1520		1840	

aIntercooler required.

(a) Blade 4.

Cap, welded
at tip of
trailing-edge
passage

Radial groove

Cooling-air
flow
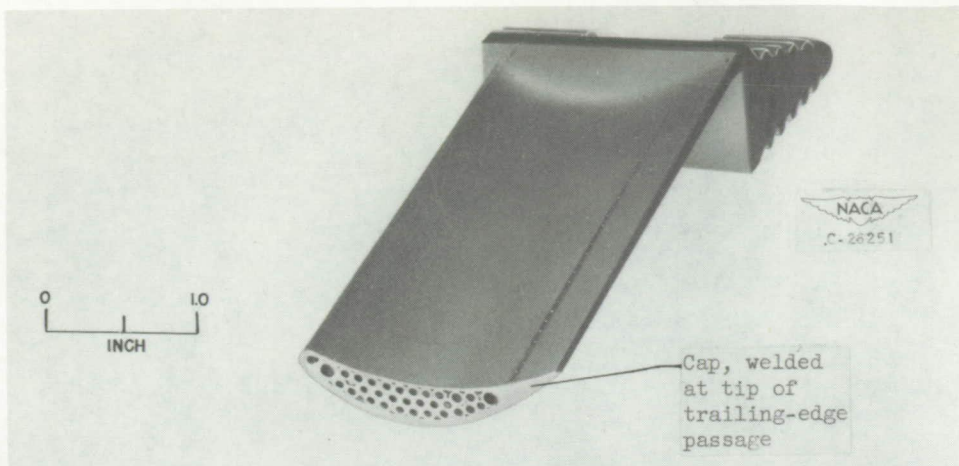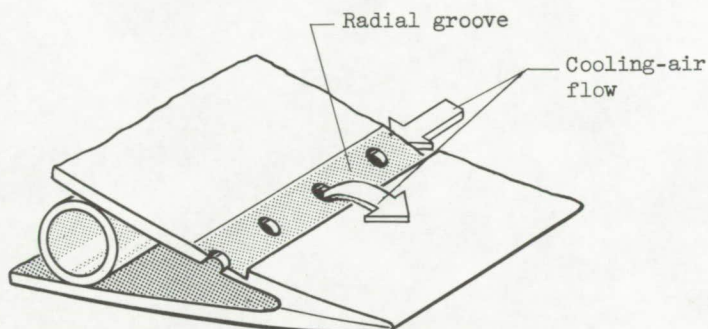
(b) Trailing-edge section of blades 4 and 5.

Cap, welded
at tip of
trailing-edge
passage

Plugged tubes
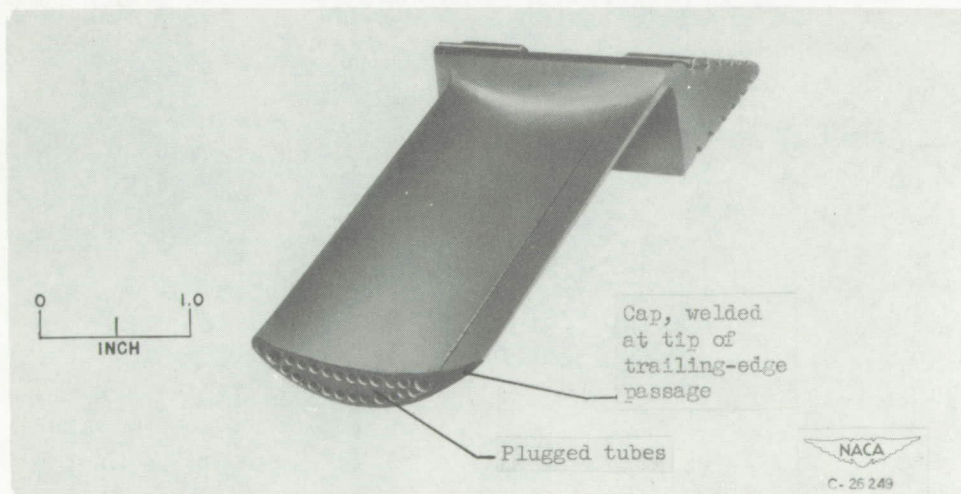
(c) Blade 5.

Figure 1.   Views of cooled turbine blades 4 and 5 with enlarged trailing-edge section.

(a) Leading-edge section.

(b) Blade 6.

(c) Trailing-edge section.
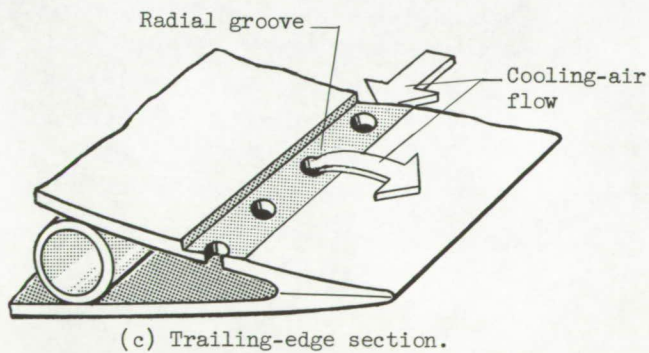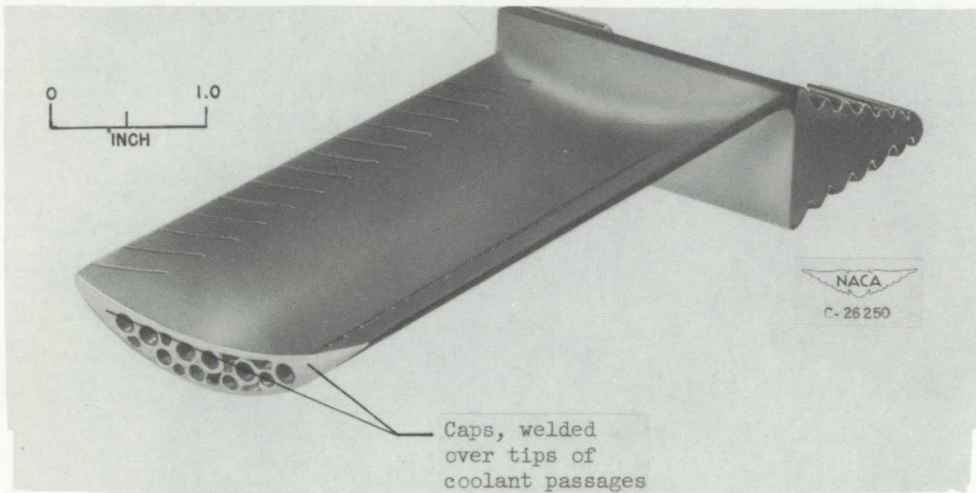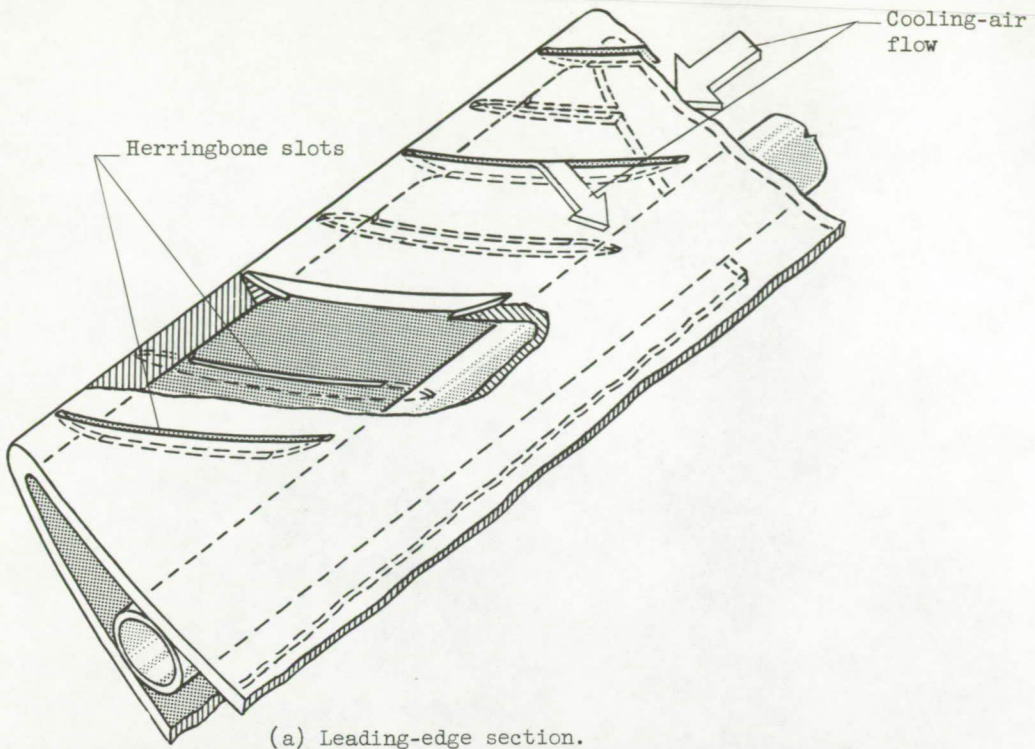
Figure 2. - Cooled turbine blade 6 with enlarged views of the leading- and trailing-edge sections.
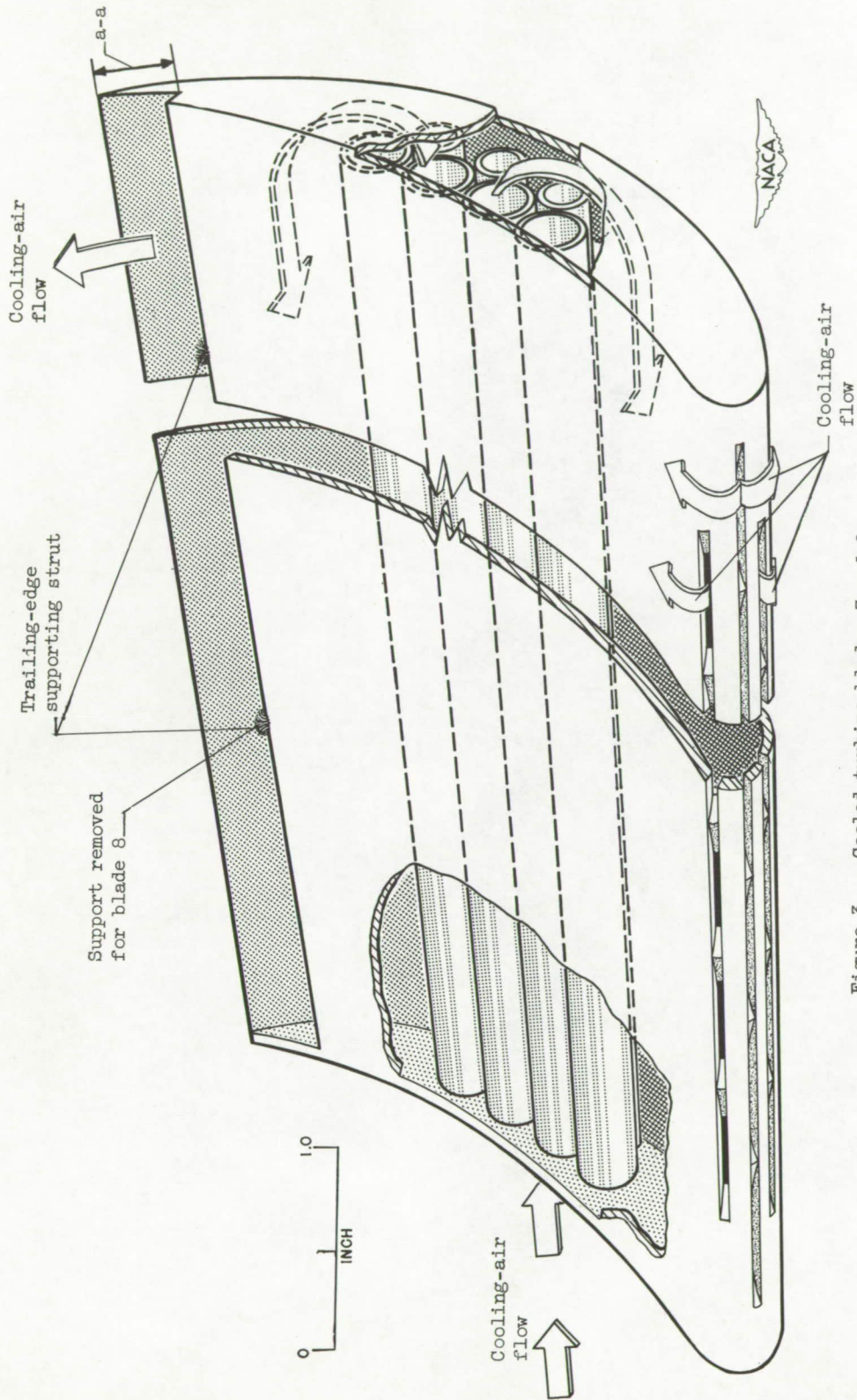
Figure 3. - Cooled turbine blades 7 and 8.
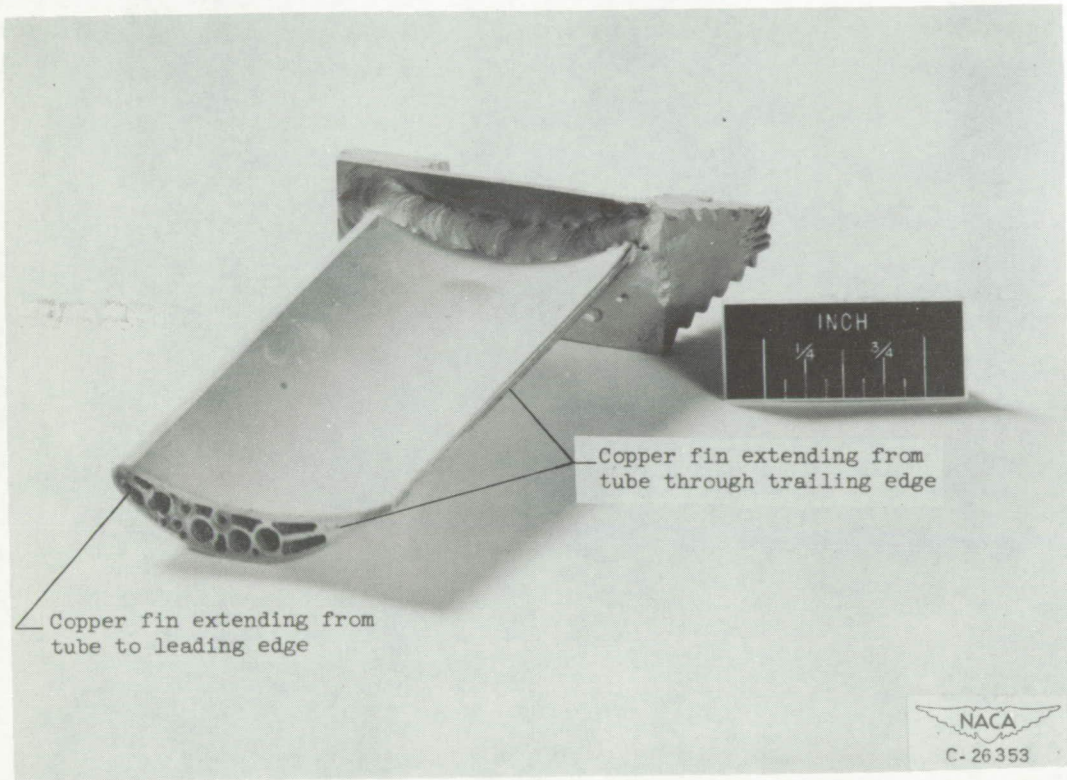
Figure 4. - Cooled turbine blade 9.
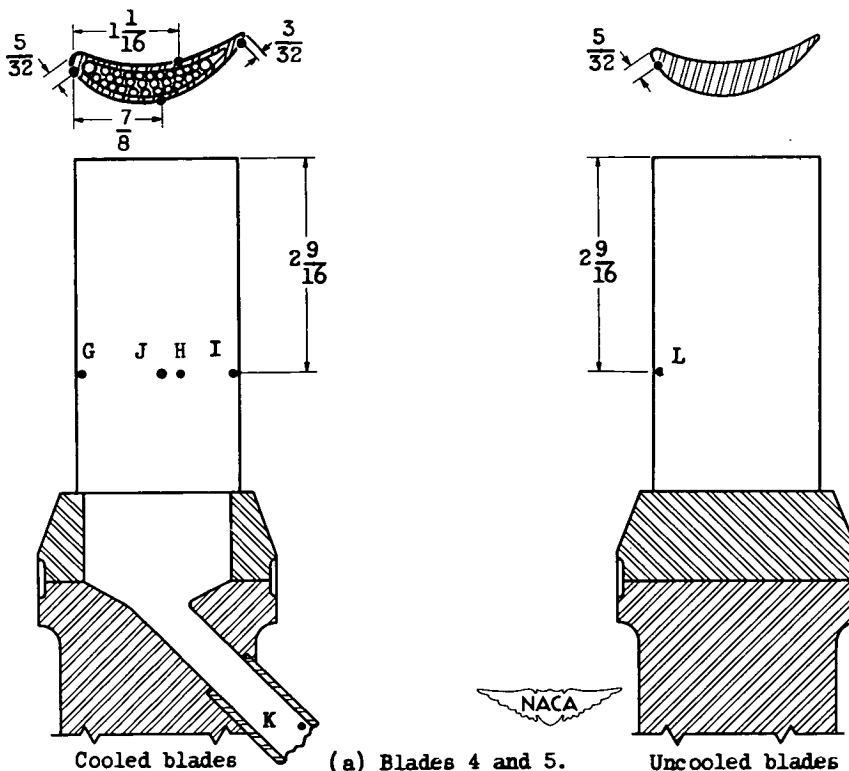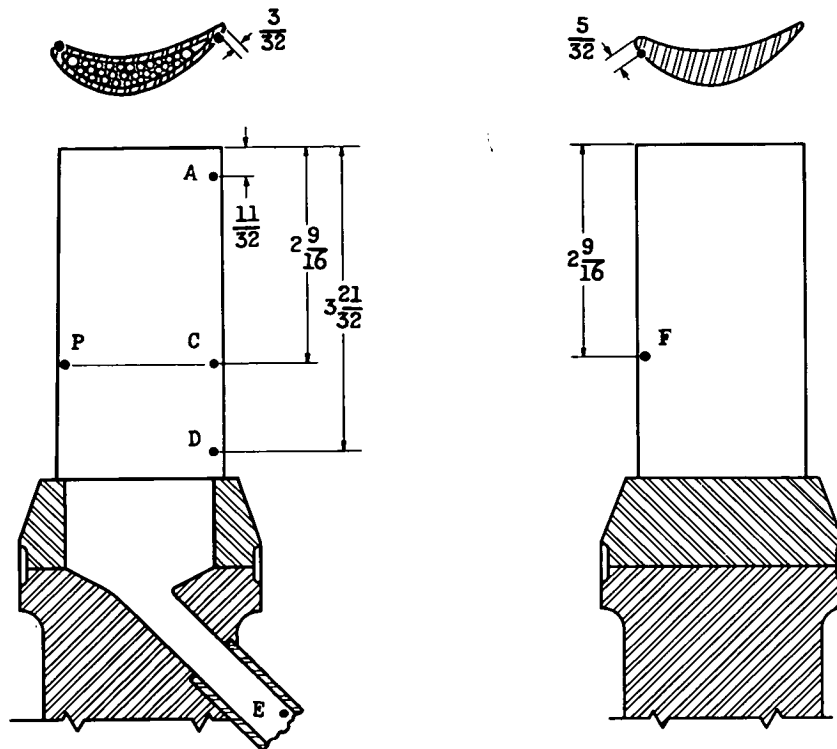
Cooled blades   (a) Blades 4 and 5.   Uncooled blades

Figure 5. - Schematic diagram of thermocouple locations on cooled and uncooled blades investigated. Dimensions in inches.

Cooled blades (b) Blade 6. Uncooled blades
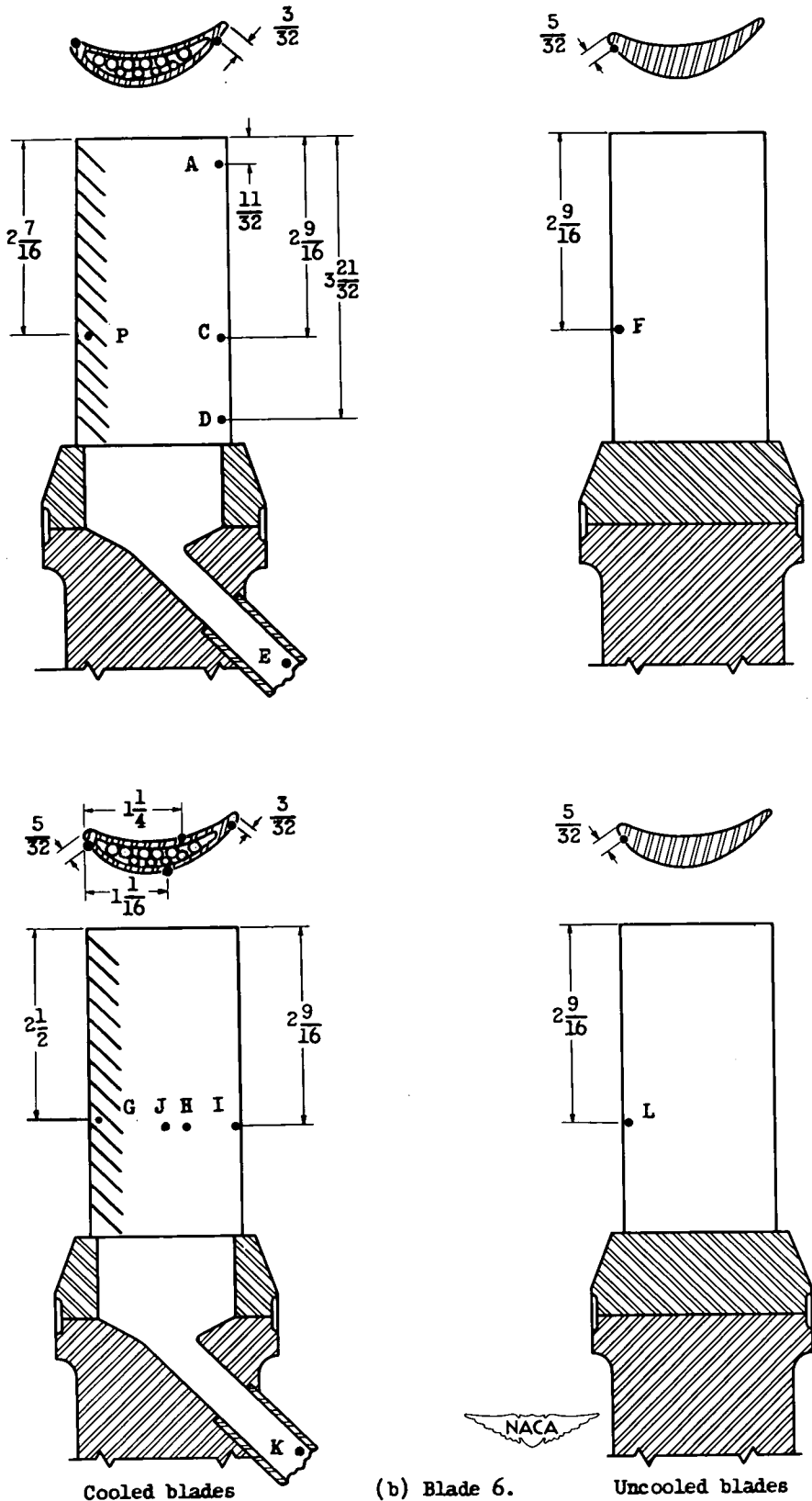
Figure 5. - Continued. Schematic diagram of thermocouple locations on cooled and uncooled blades investigated. Dimensions in inches.

Cooled blades   (c) Blades 7 and 8.   Uncooled blades

Figure 5. - Continued. Schematic diagram of thermocouple locations on cooled and uncooled blades investigated. Dimensions in inches.

Cooled blades   (d) Blade 9.   Uncooled blades
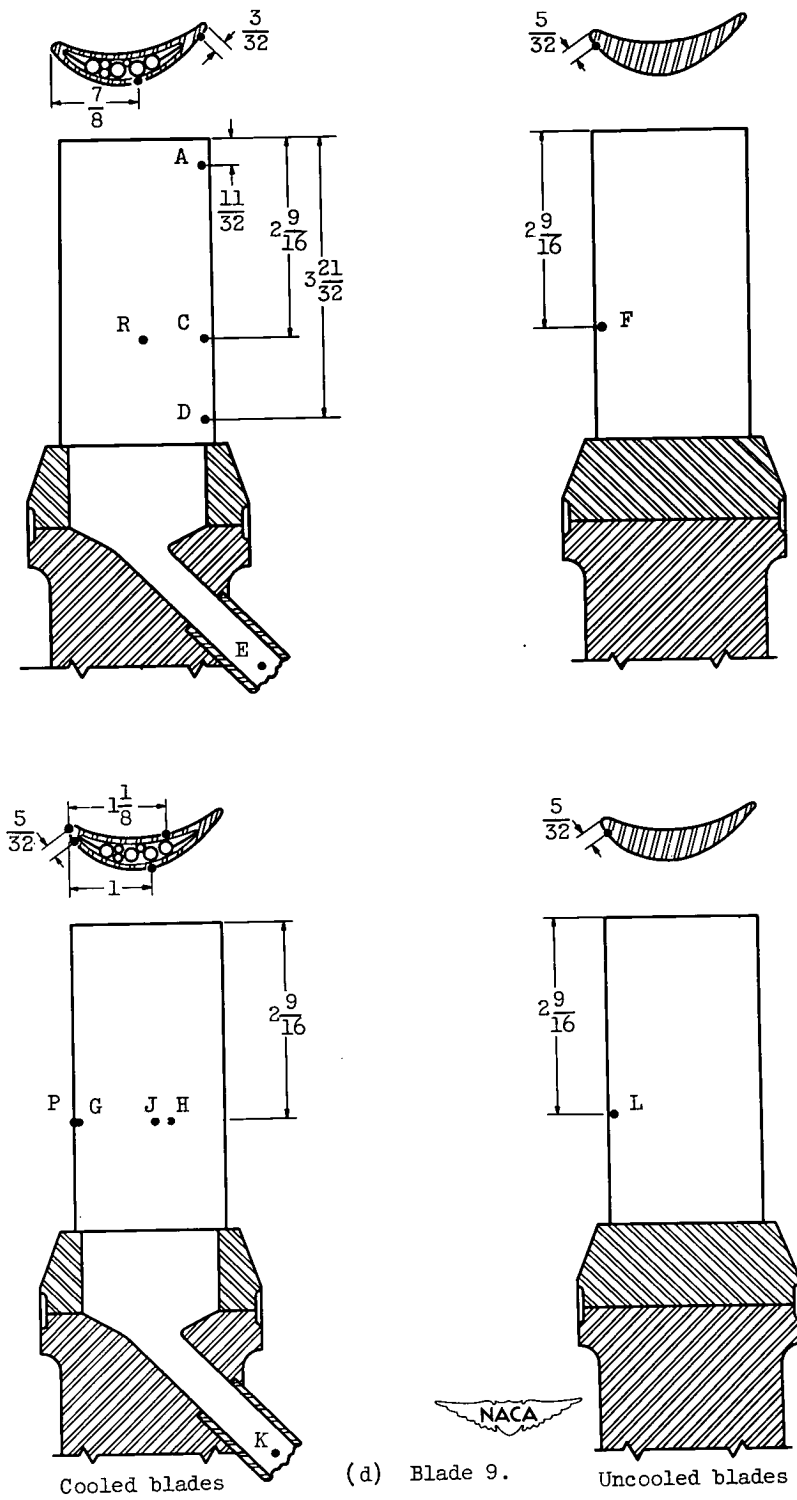
Figure 5. - Concluded. Schematic diagram of thermocouple locations on cooled and uncooled
blades investigated. Dimensions in inches.
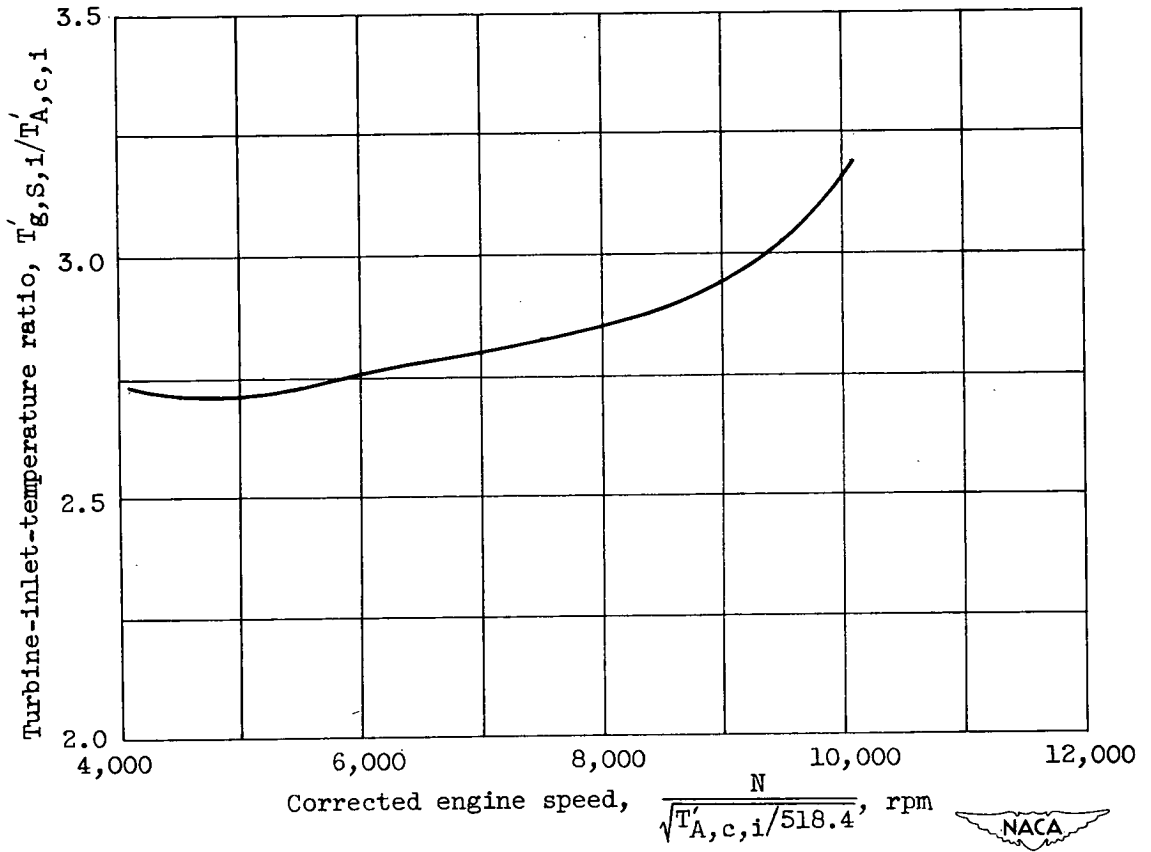
Figure 6. - Variation of turbine-inlet-temperature ratio with corrected engine speed.

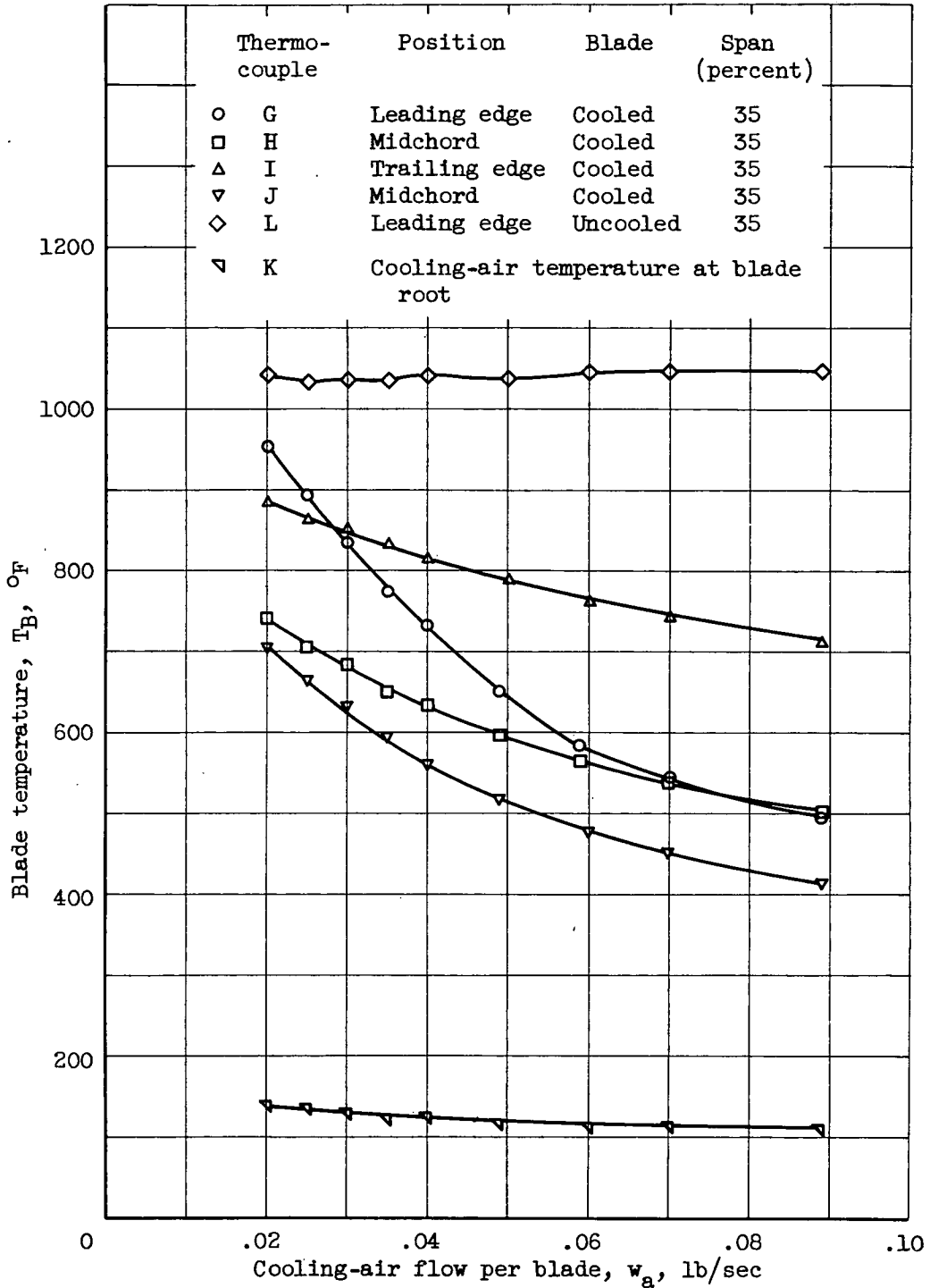|	Thermo-couple	Position	Blade	Span (percent)
△	C	Trailing edge	Cooled	35
▽	D	Trailing edge	Cooled	91
▼	P	Leading edge	Cooled	35
◇	L	Leading edge	Uncooled	35
◁	E	Cooling-air temperature at blade root		
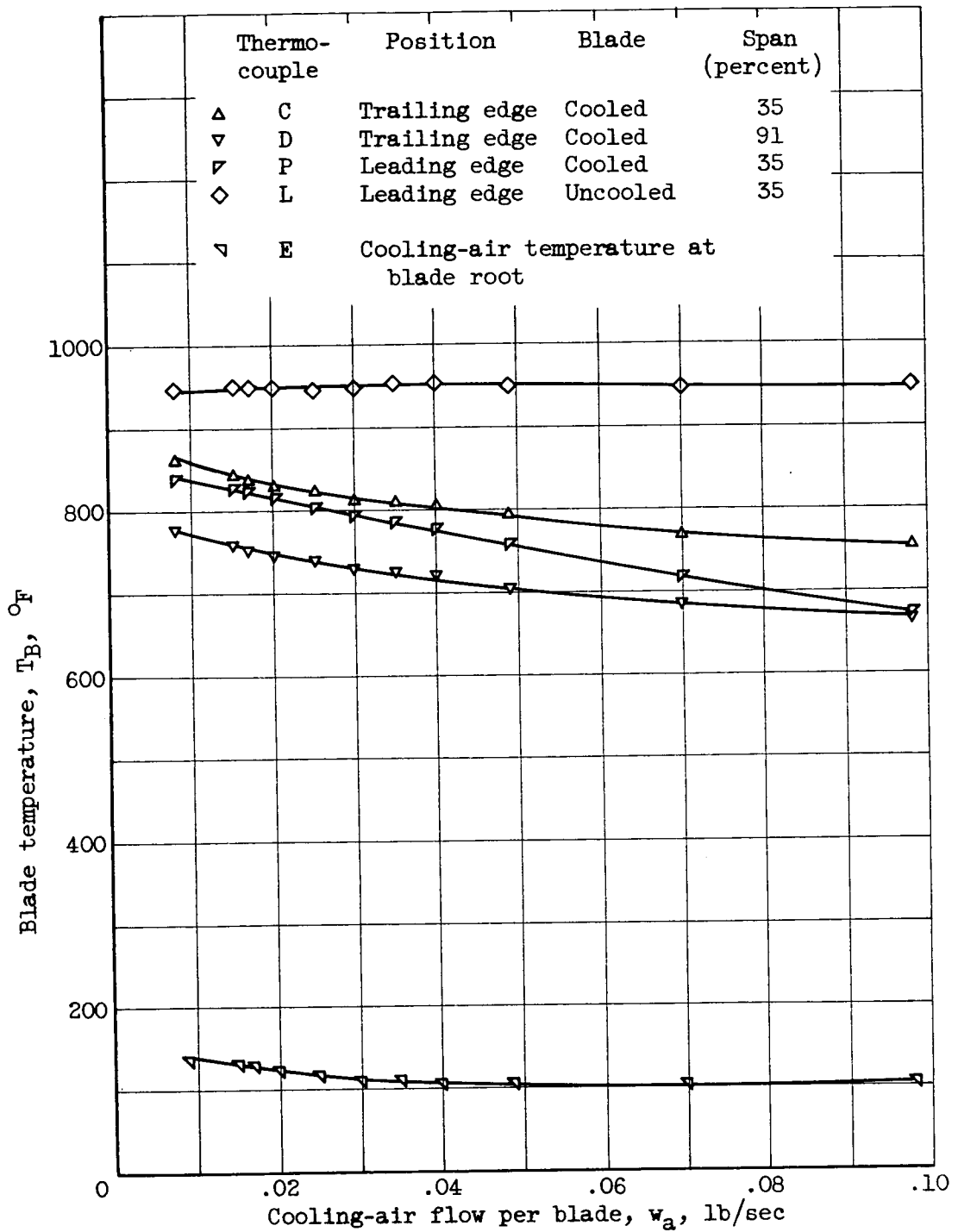
(a) Thermocouples C, D, P, E, and L.

Figure 7. - Effect of cooling-air-flow rate on blade and cooling-air temperatures for blade 4 at engine speed of 9000 rpm.

	Thermo-couple	Position	Blade	Span (percent)
O	G	Leading edge	Cooled	35
□	H	Midchord	Cooled	35
△	I	Trailing edge	Cooled	35
▽	J	Midchord	Cooled	35
◇	L	Leading edge	Uncooled	35
▽	K	Cooling-air temperature at blade root		
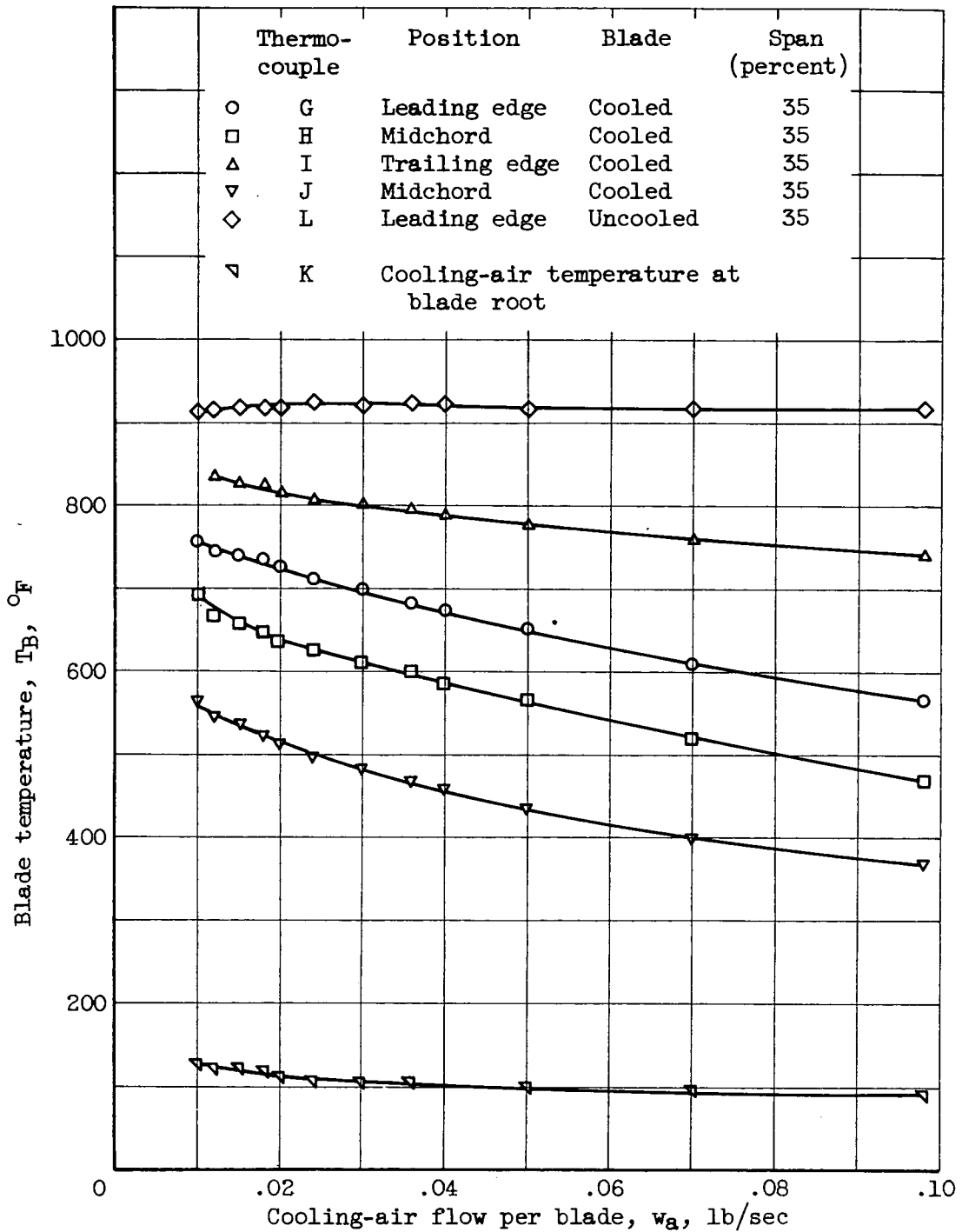
(b) Thermocouples G, H, I, J, K, and L.

Figure 7. - Concluded. Effect of cooling-air-flow rate on blade and cooling-air temperatures for blade 4 at engine speed of 9000 rpm.
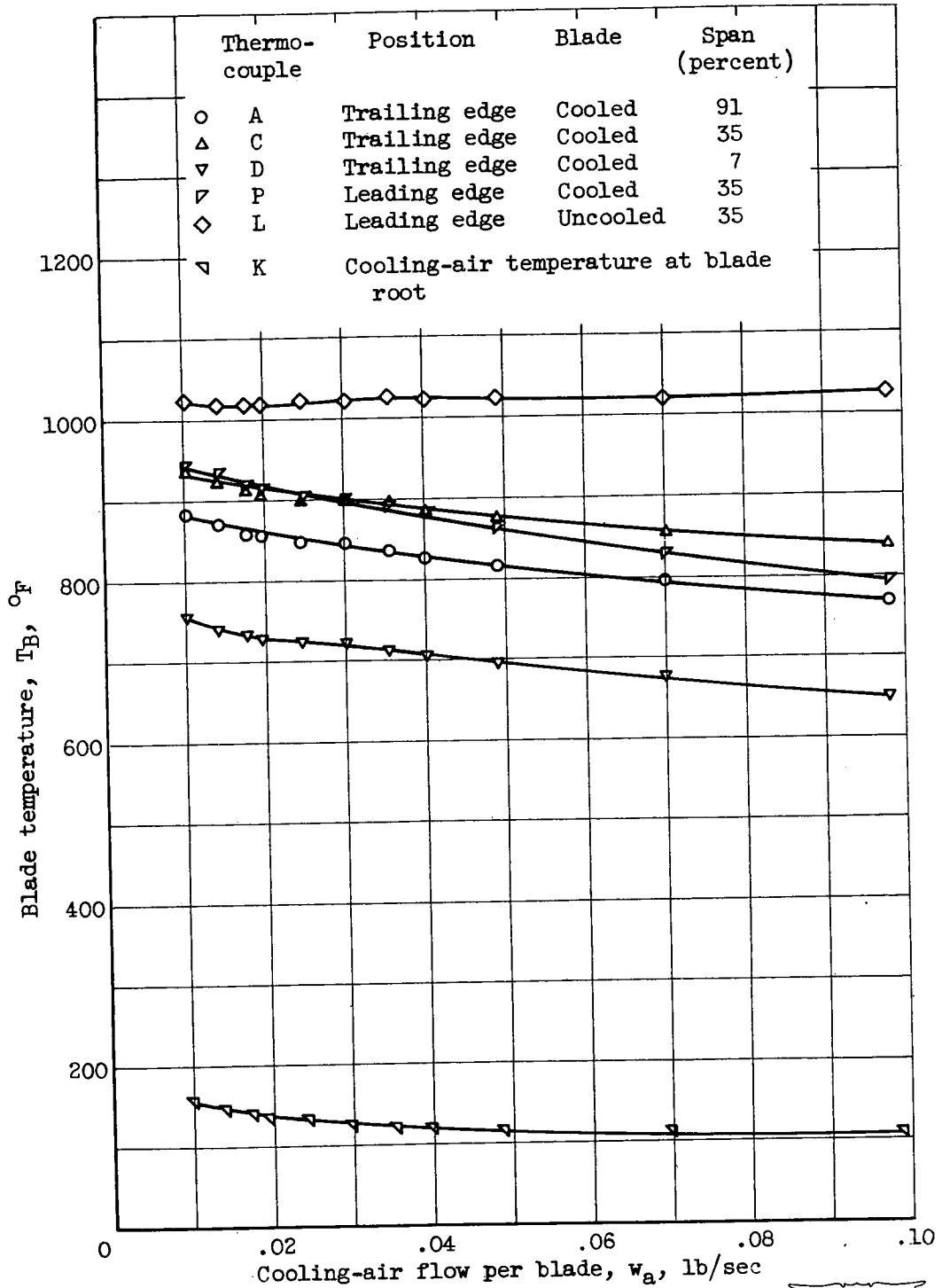
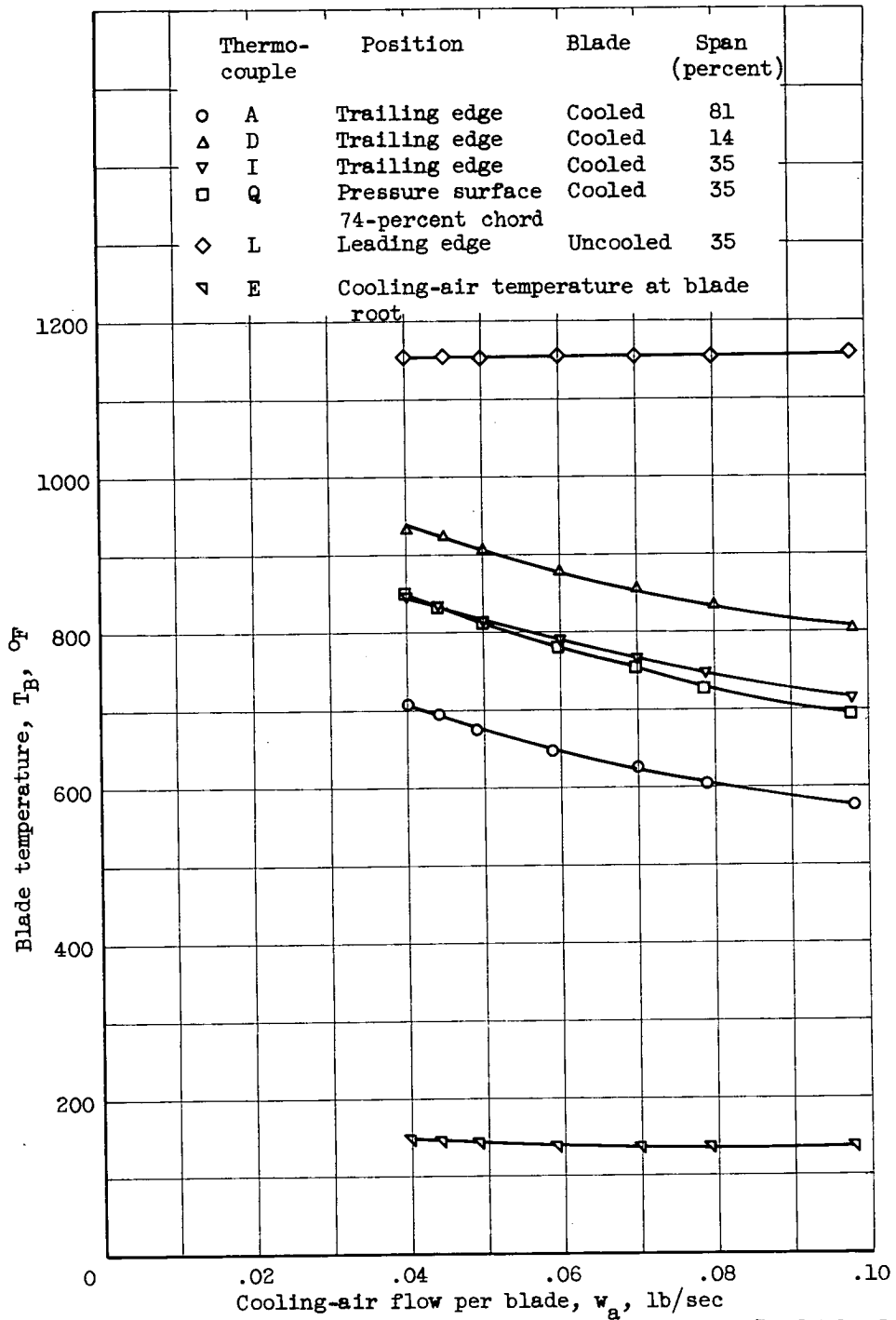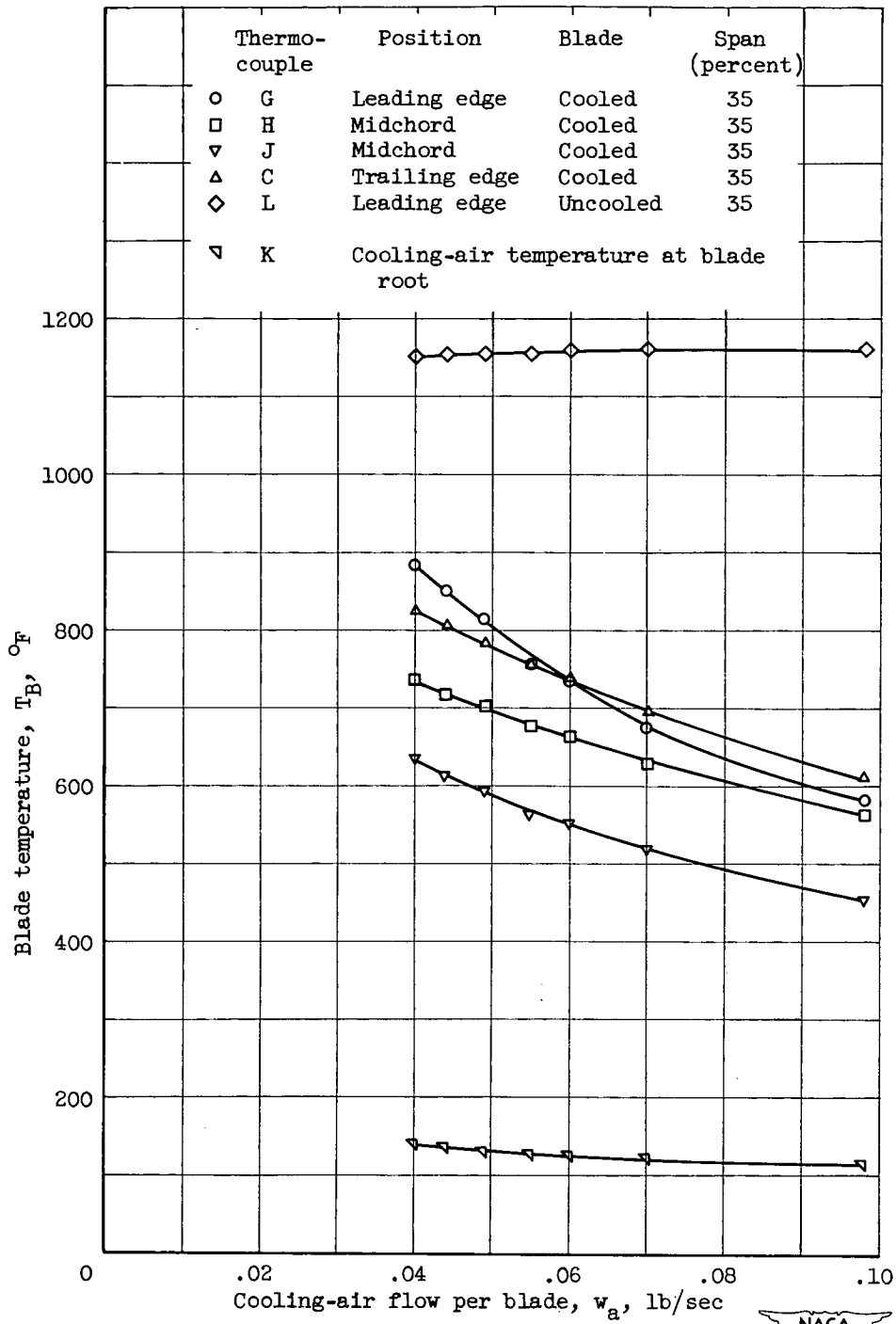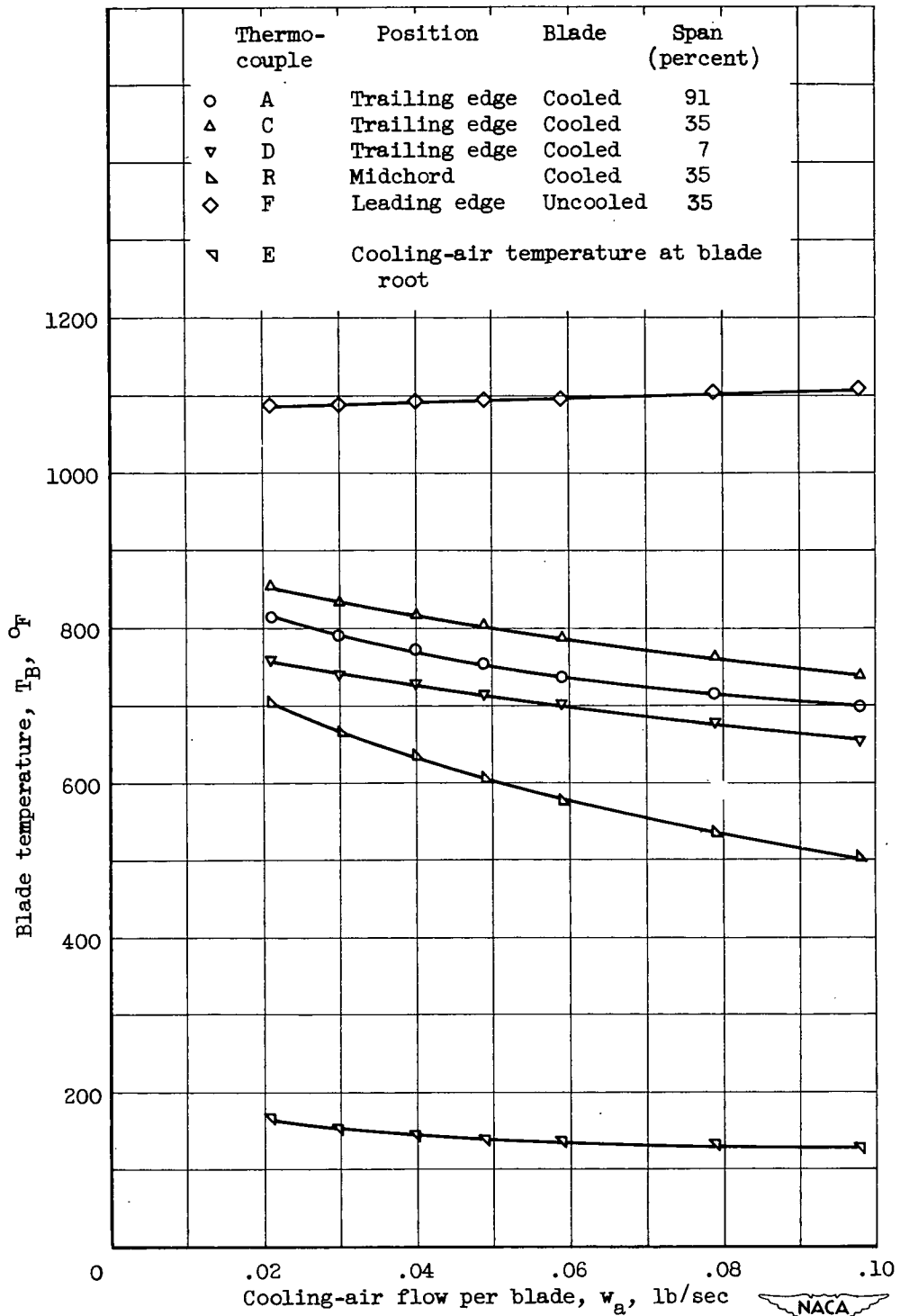(a) Thermocouples A, C, D, P, K, and L.

Figure 8. - Effect of cooling-air-flow rate on blade and
cooling-air temperatures for blade 5 at engine speed
of 10,000 rpm.

Thermo-couple		Position	Blade	Span (percent)
o	G	Leading edge	Cooled	35
□	H	Midchord	Cooled	35
△	I	Trailing edge	Cooled	35
▽	J	Midchord	Cooled	35
◇	L	Leading edge	Uncooled	35
⊴	K	Cooling-air temperature at blade root		

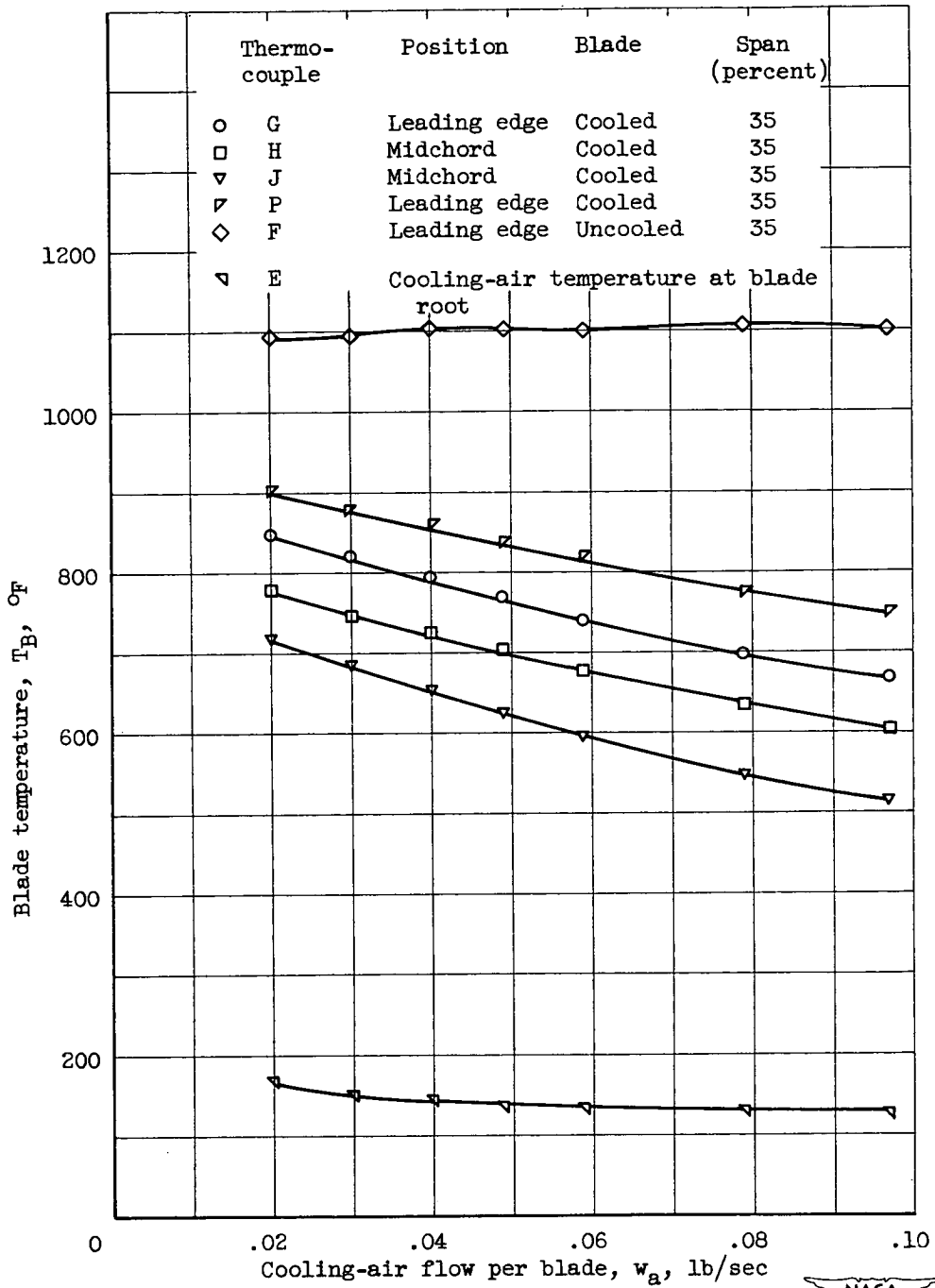Blade temperature, T_B, °F

Cooling-air flow per blade, w_a, lb/sec
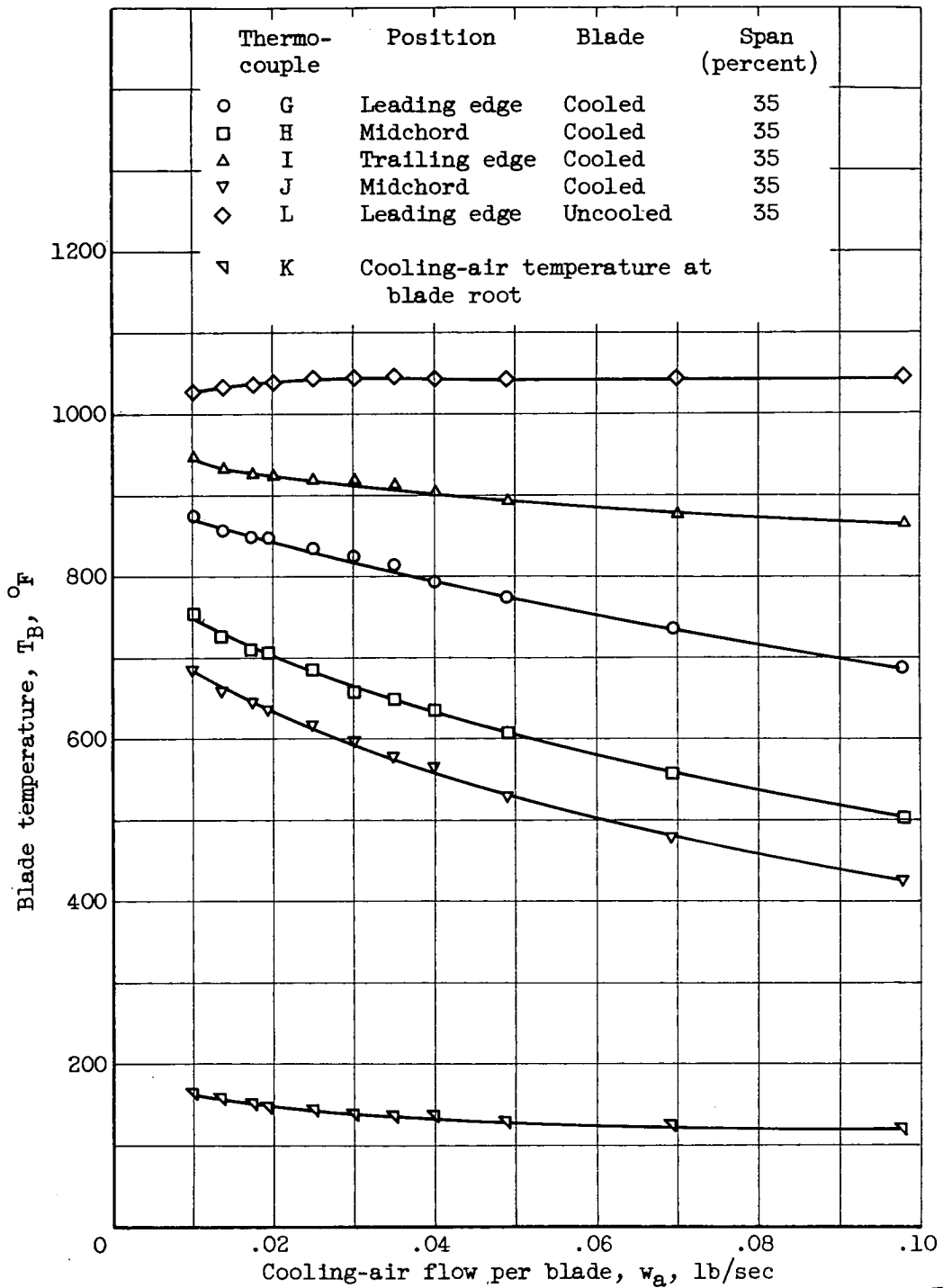
(b) Thermocouples G, H, I, J, K, and L.

Figure 8. - Concluded. Effect of cooling-air-flow rate on blade and cooling-air temperatures for blade 5 at engine speed of 10,000 rpm.

Thermo-couple		Position	Blade	Span (percent)
○	A	Trailing edge	Cooled	91
△	C	Trailing edge	Cooled	35
▽	D	Trailing edge	Cooled	7
▼	P	Leading edge	Cooled	35
◇	L	Leading edge	Uncooled	35
◁	E	Cooling-air temperature at blade root		
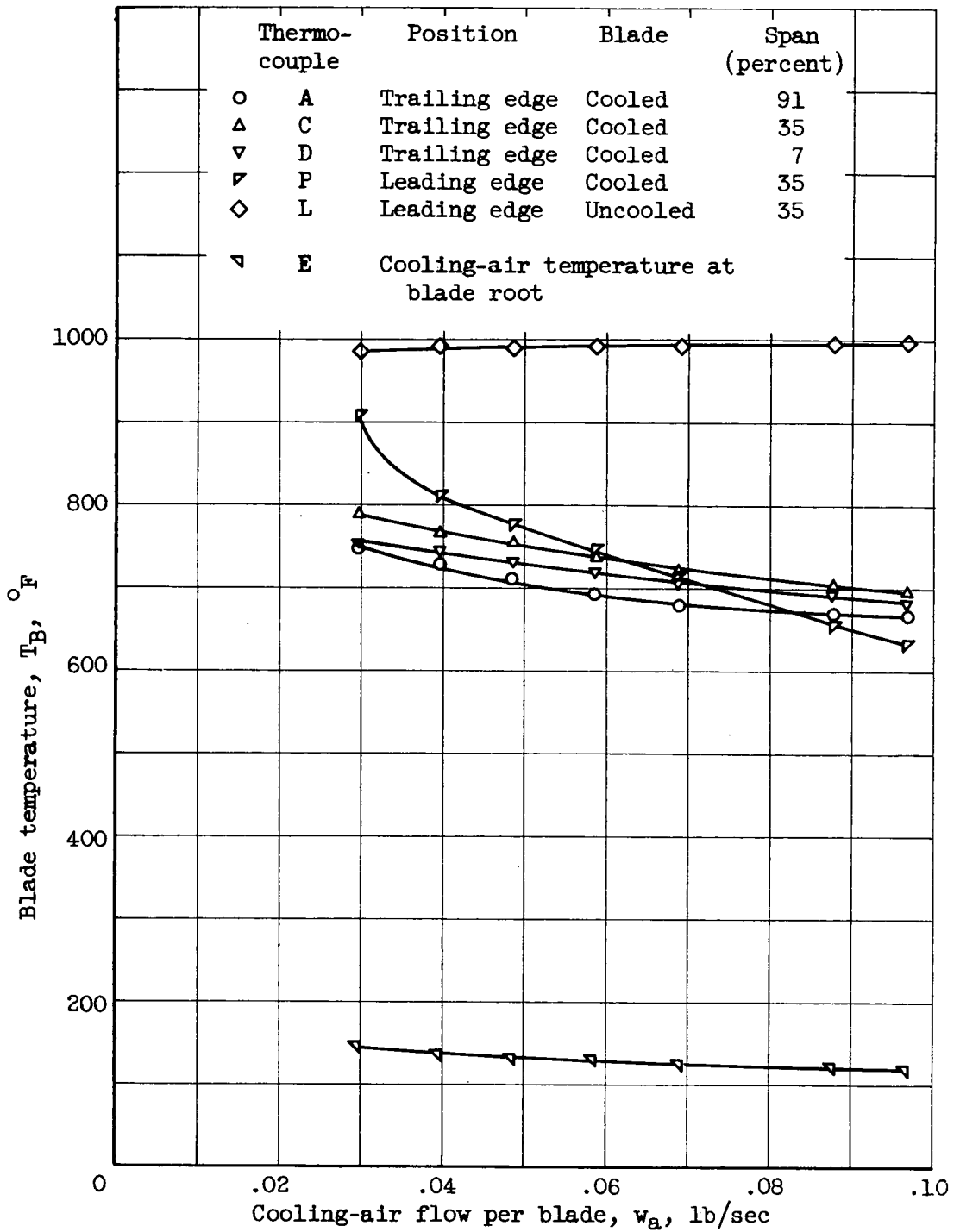
(a) Thermocouples A, C, D, P, E, and L.
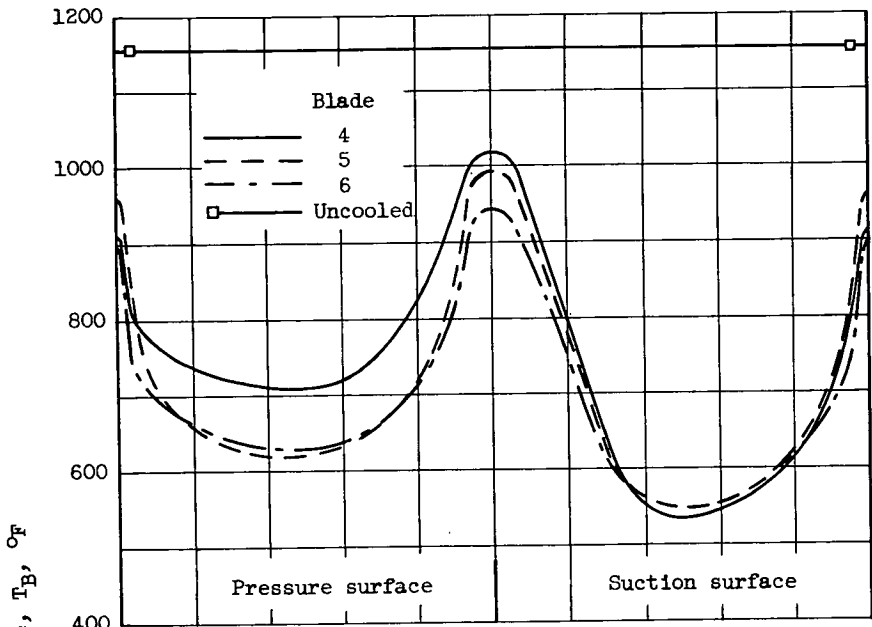
Figure 9. - Effect of cooling-air-flow rate on blade and cooling-air temperatures for blade 6 at engine speed of 9000 rpm.

| Thermo-couple		Position	Blade	Span (percent)
o	G	Leading edge	Cooled	35
□	H	Midchord	Cooled	35
△	I	Trailing edge	Cooled	35
▽	J	Midchord	Cooled	35
◇	L	Leading edge	Uncooled	35
◁	K	Cooling-air temperature at blade root		
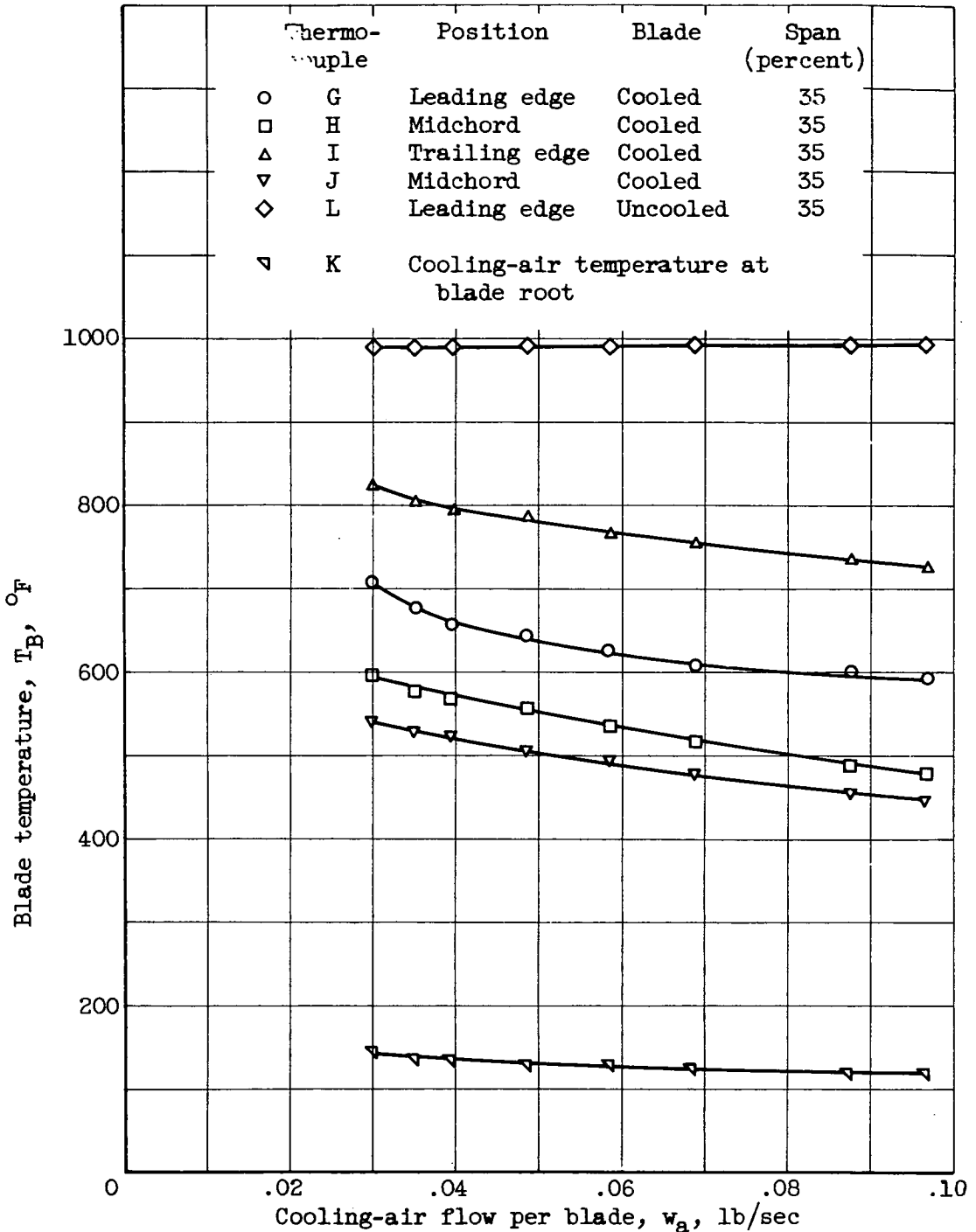
(b) Thermocouples G, H, I, J, K, and L.

Figure 9. - Concluded. Effect of cooling-air-flow rate on blade and cooling-air temperatures for blade 6 at engine speed of 9000 rpm.
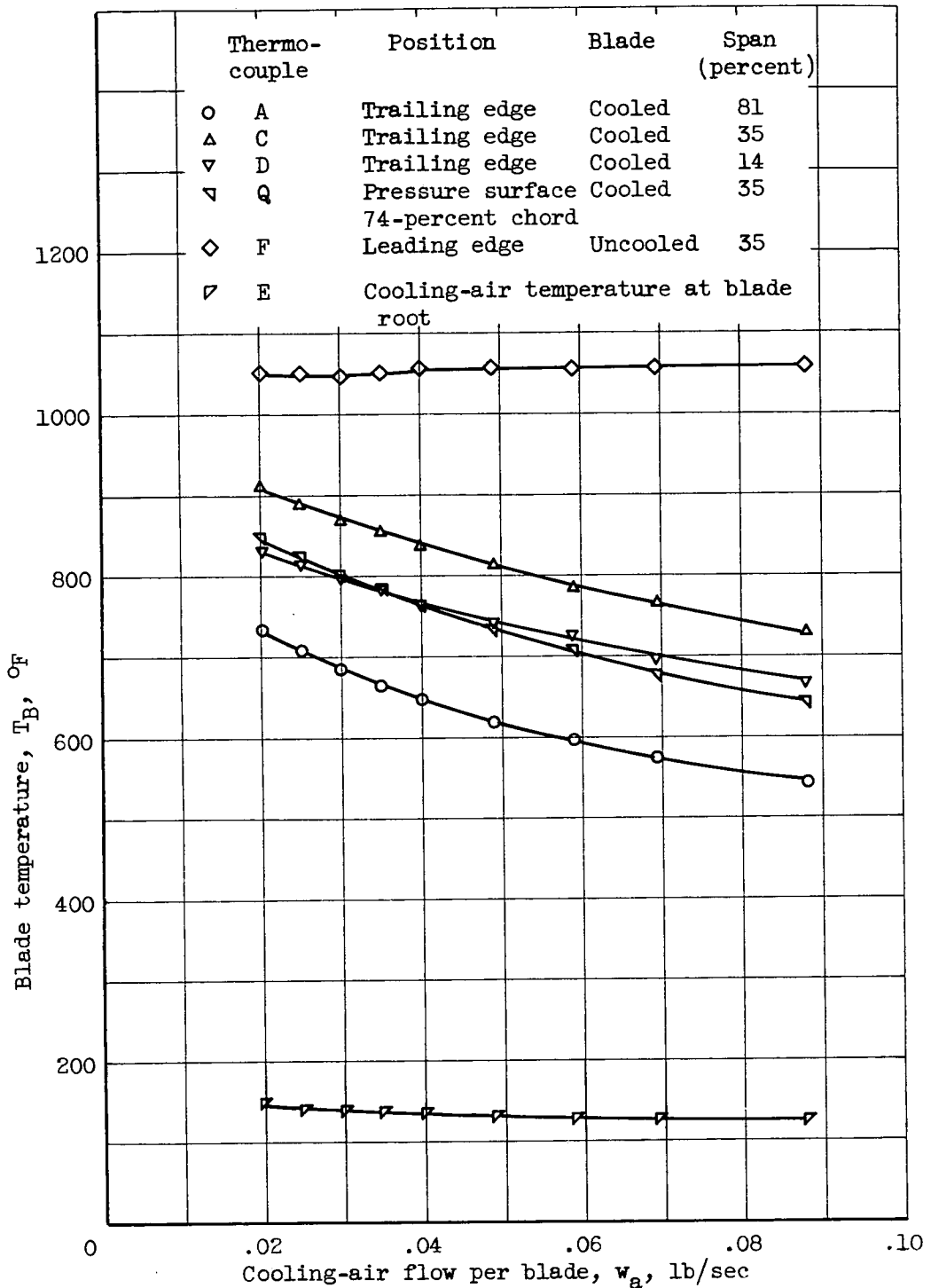
(a) Thermocouples A, C, D, Q, E, and F.

Figure 10. - Effect of cooling-air-flow rate on blade and
cooling-air temperatures for blade 7 at an engine speed
of 9000 rpm.

	Thermo-couple	Position	Blade	Span (percent)
○	G	Leading edge	Cooled	35
□	H	Midchord	Cooled	35
△	I	Trailing edge	Cooled	35
▽	J	Midchord	Cooled	35
◇	L	Leading edge	Uncooled	35
◁	K	Cooling-air temperature at blade root		

(b) Thermocouples G, H, I, J, K, and L.

Figure 10. - Concluded. Effect of cooling-air-flow rate on blade and cooling-air temperatures for blade 7 at engine speed of 9000 rpm.

(a) Thermocouples A, D, I, Q, E, and L.

Figure 11. - Effect of cooling-air-flow rate on blade and
cooling-air temperatures for blade 8 at engine speed of
10,000 rpm.

Thermo-couple		Position	Blade	Span (percent)
○	G	Leading edge	Cooled	35
□	H	Midchord	Cooled	35
▽	J	Midchord	Cooled	35
△	C	Trailing edge	Cooled	35
◇	L	Leading edge	Uncooled	35
◁	K	Cooling-air temperature at blade root		

(b) Thermocouples G, H, J, C, K, and L.

Figure 11. - Concluded. Effect of cooling-air-flow rate on blade and cooling-air temperatures for blade 8 at engine speed of 10,000 rpm.

Thermo-couple	Position	Blade	Span (percent)
○ A	Trailing edge	Cooled	91
△ C	Trailing edge	Cooled	35
▽ D	Trailing edge	Cooled	7
◗ R	Midchord	Cooled	35
◇ F	Leading edge	Uncooled	35
◁ E	Cooling-air temperature at blade root		

(a) Thermocouples A, C, D, R, E, and F.

Figure 12. - Effect of cooling-air-flow rate on blade and cooling-air temperatures for blade 9 at engine speed of 10,000 rpm.

(b)   Thermocouples G, H, J, P, E, and F.

Figure 12. - Concluded. Effect of cooling-air-flow rate on blade
and cooling-air temperatures for blade 9 at engine speed of
10,000 rpm.

(a) Blades 4, 5, and 6.
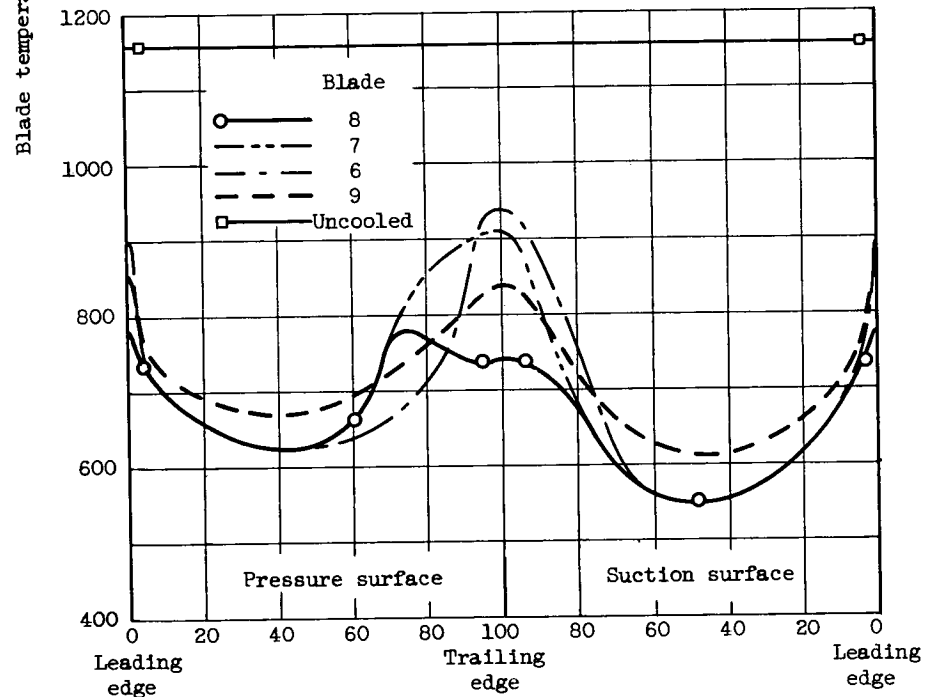
(b) Blades 6, 7, 8, and 9.

Figure 13. - Comparison of chordwise blade temperatures for blades
investigated. Engine speed, 10,000 rpm; ratio of cooling-air
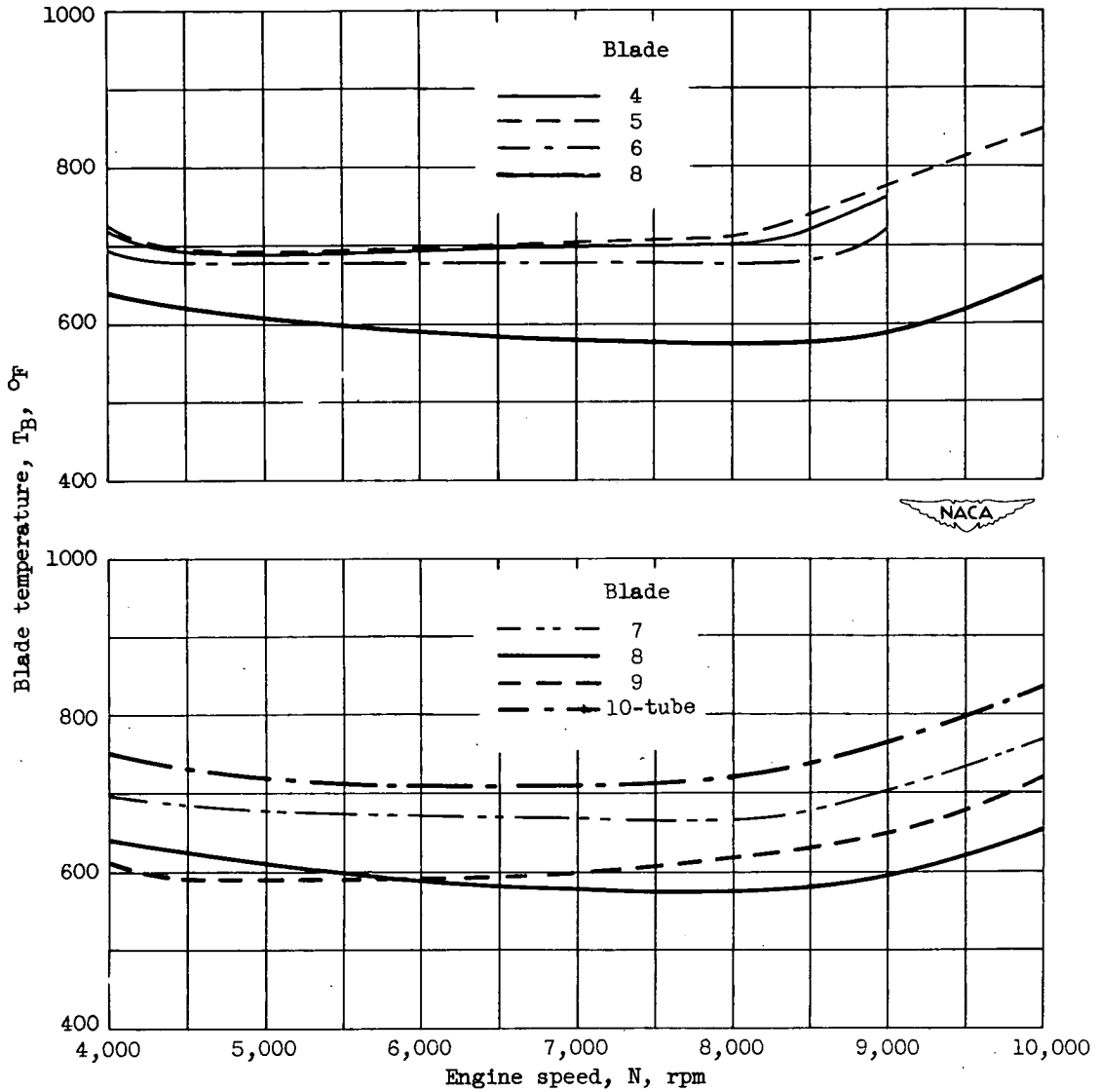flow to combustion-gas flow, 0.056; cooling-air temperature,
126° F.
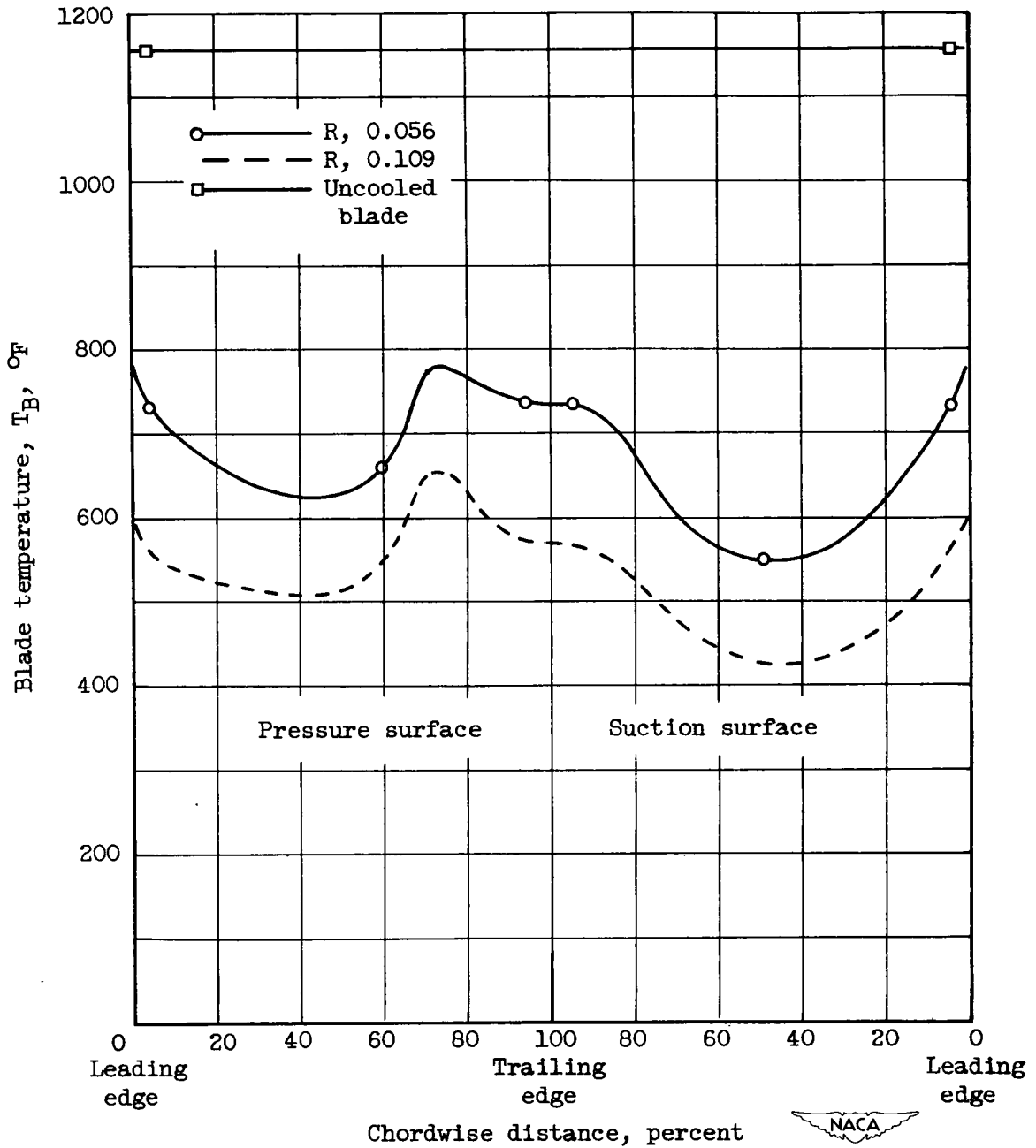
Figure 14. - Effect of ratio of cooling-air-flow rate to combustion-
gas-flow rate on blade temperatures of blade 8. Engine speed,
10,000 rpm; cooling-air temperature, 126° F.
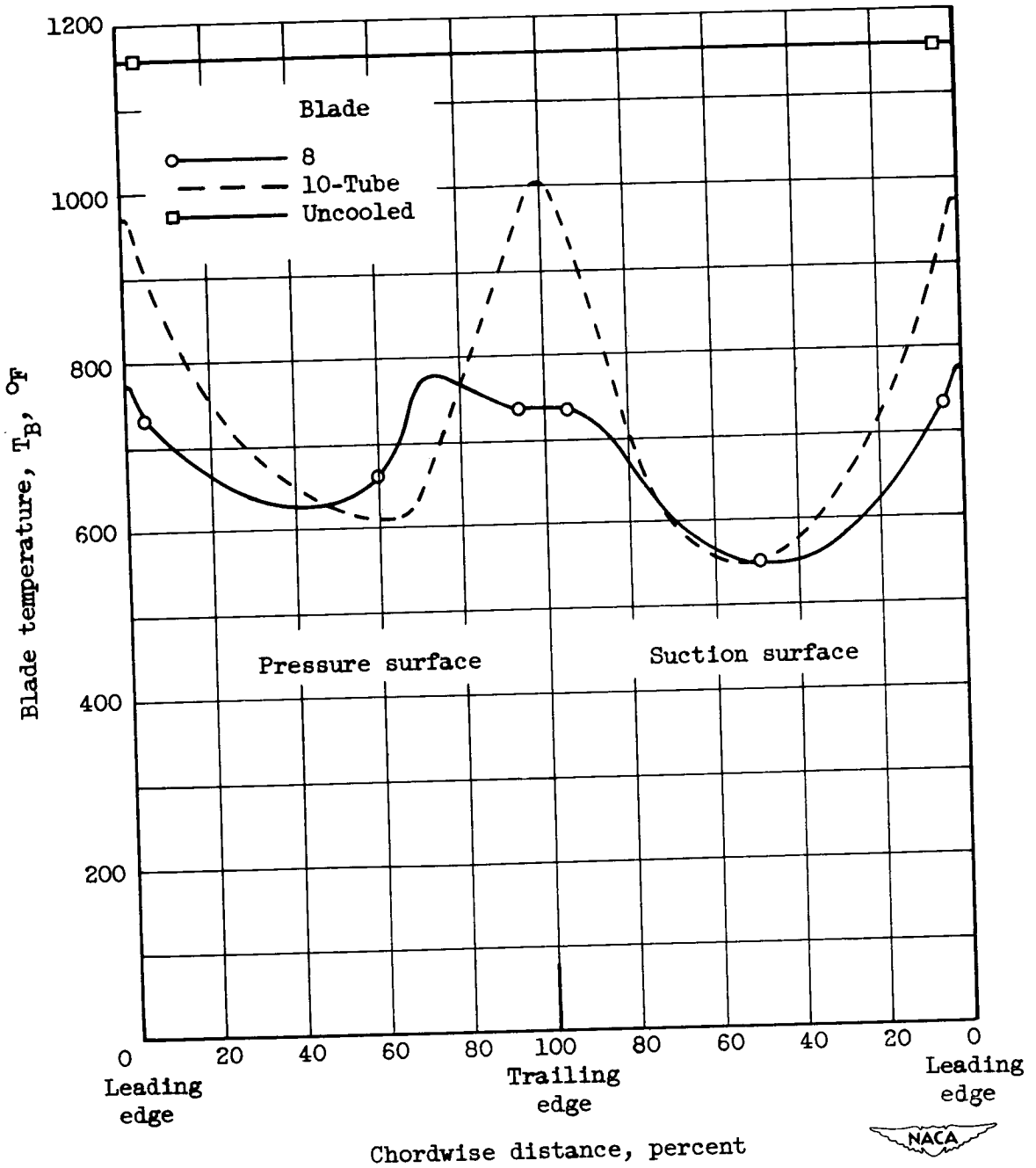
Figure 15. - Comparison of chordwise blade-temperature distributions of blade 8 and 10-tube blade. Engine speed, 10,000 rpm; ratio of cooling-air flow to combustion-gas flow, 0.056; cooling-air temperature, 126° F.
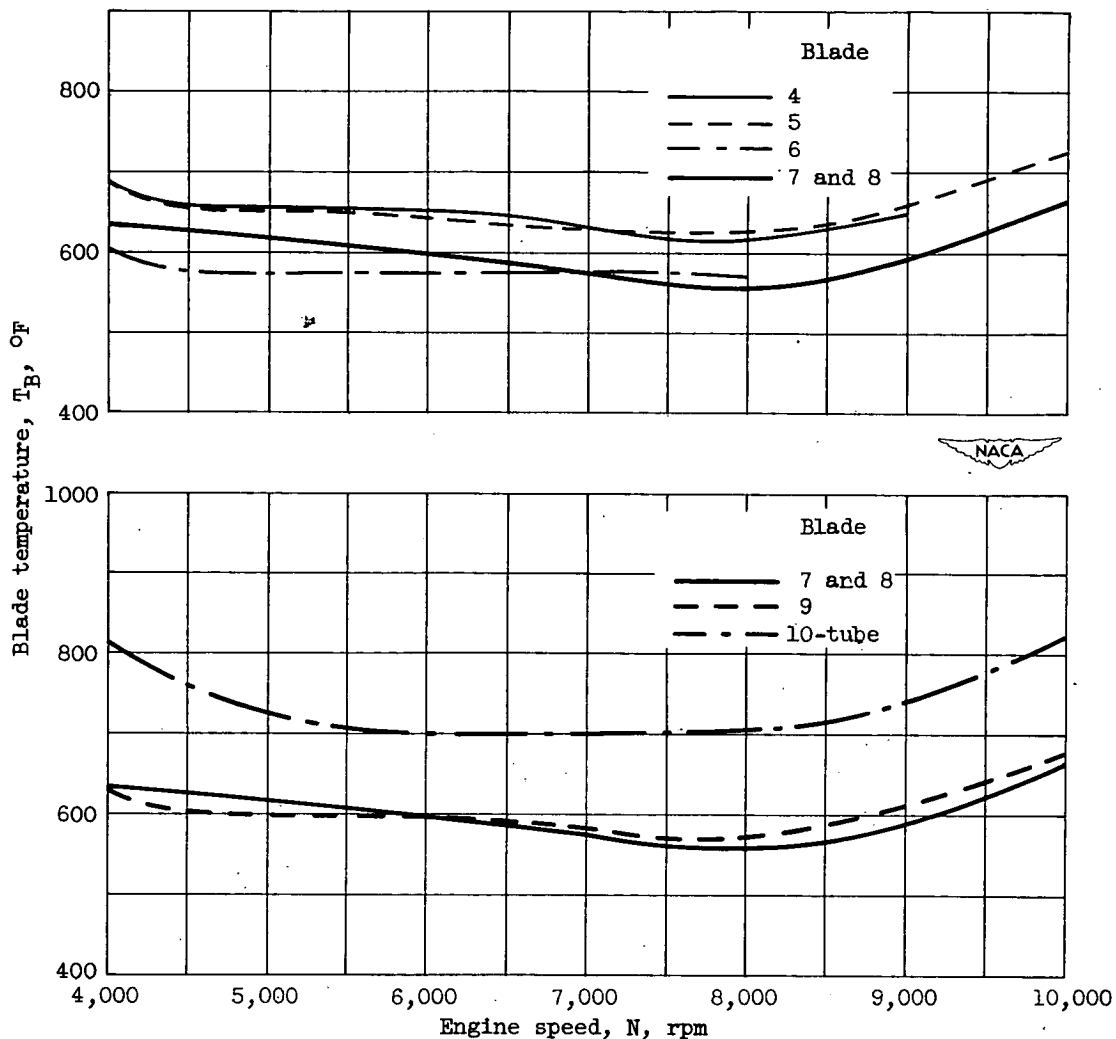
(a) Thermocouple G; leading edge; 35-percent span.

Figure 16. - Comparison of blade temperatures of blades investigated and
10-tube blade over range of engine speed for standard inlet conditions.
Ratio of cooling-air flow to combustion-gas flow, 0.05; effective gas
temperature and cooling-air temperature given in reference 2.
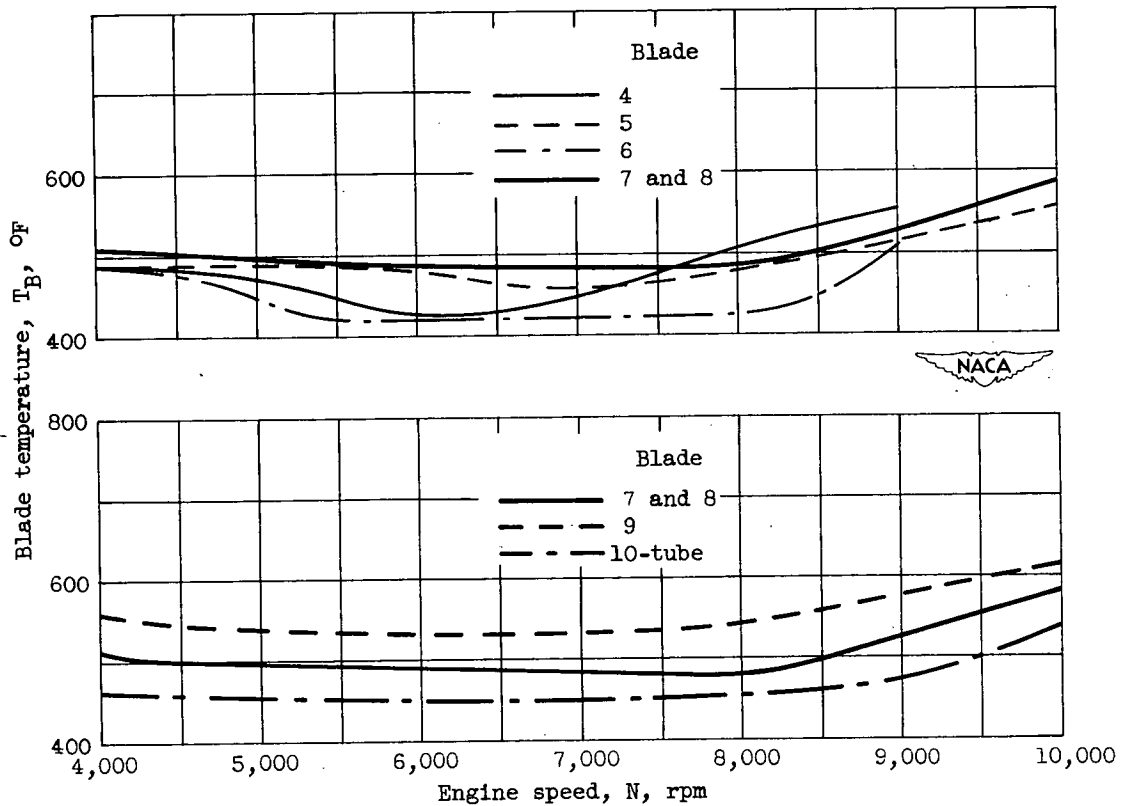
(b) Thermocouple H; pressure surface; 35-percent span.

Figure 16. - Continued. Comparison of blade temperatures of blades investi-
gated and 10-tube blade over range of engine speed for standard inlet
conditions. Ratio of cooling-air flow to combustion-gas flow, 0.05;
effective gas temperature and cooling-air temperature given in reference 2.

(c) Trailing-edge thermocouple I; 35-percent span.

Figure 16. - Continued. Comparison of blade temperatures of blades investi-
gated and 10-tube blade over range of engine speed for standard inlet con-
ditions. Ratio of cooling-air flow to combustion-gas flow, 0.05; effective
gas temperature and cooling-air temperature given in reference 2.
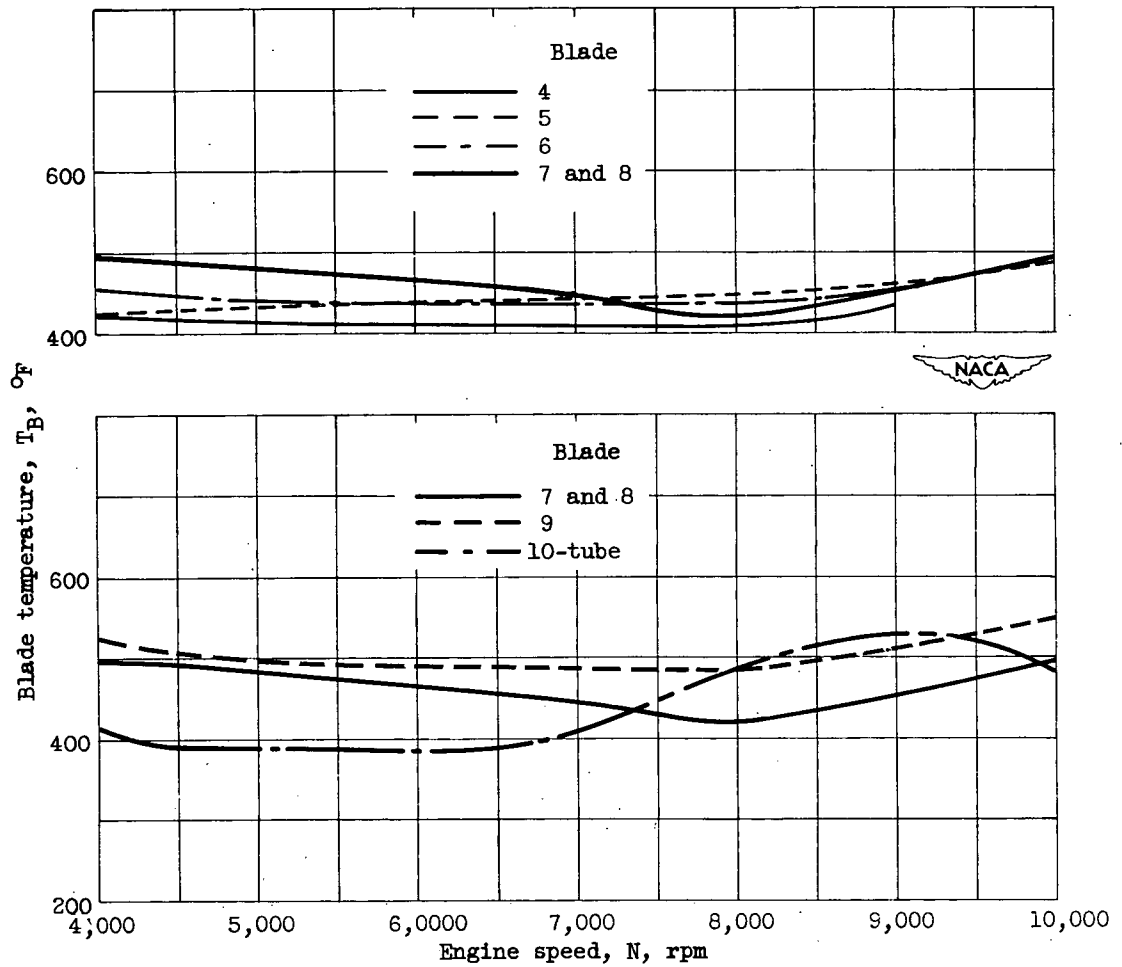
(d)   Thermocouple J; suction surface; 35-percent span.

Figure 16. - Concluded. Comparison of blade temperatures of blades investi-
gated and 10-tube blade over range of engine speed for standard inlet
conditions. Rate of cooling-air flow to combustion-gas flow, 0.05;
effective gas temperature and cooling-air temperature given in reference 2.

(a) Blade 4.

(b) Blade 5.
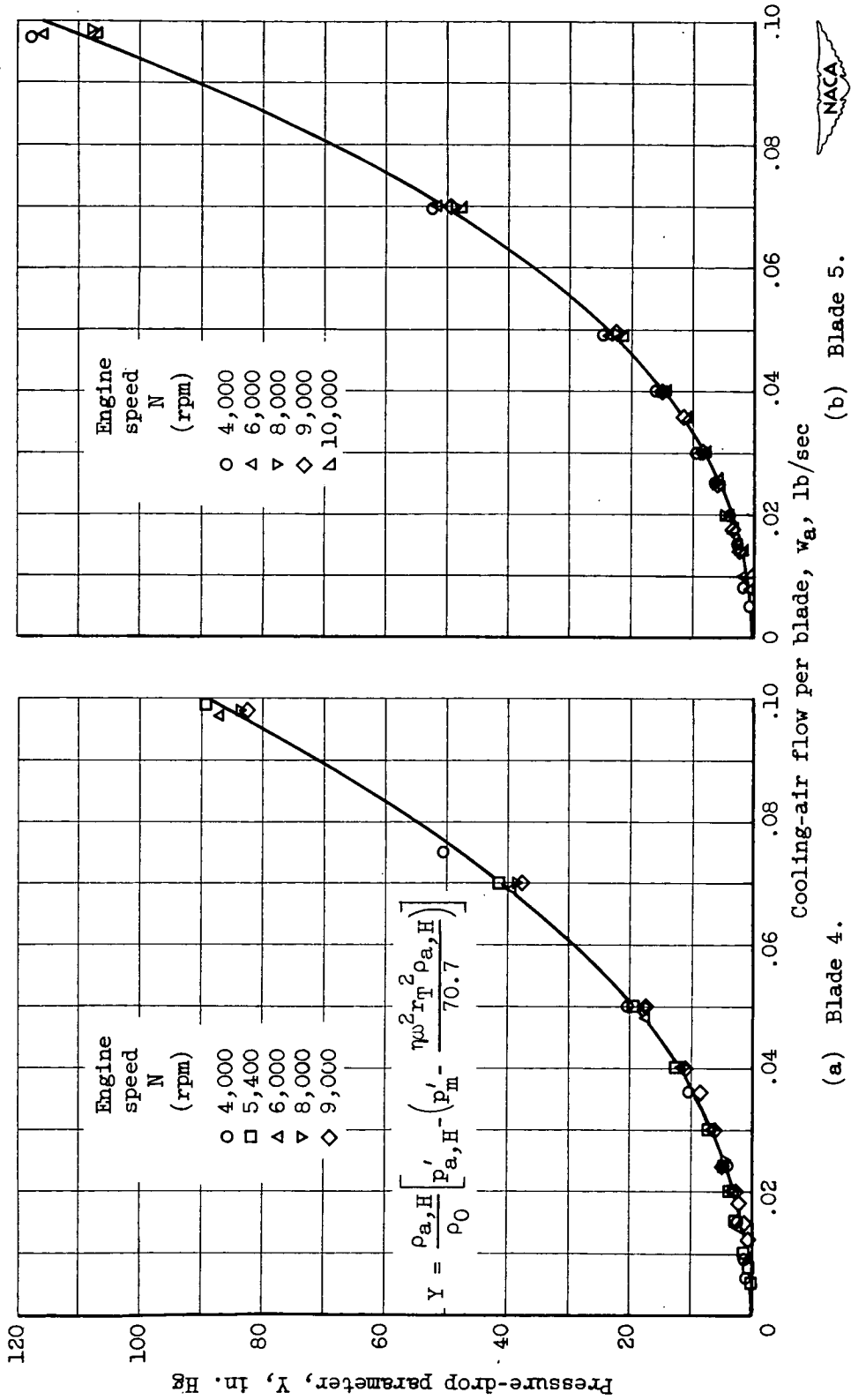
Figure 17. - Correlation of cooling-air-pressure drop from rotor hub to blade tip.
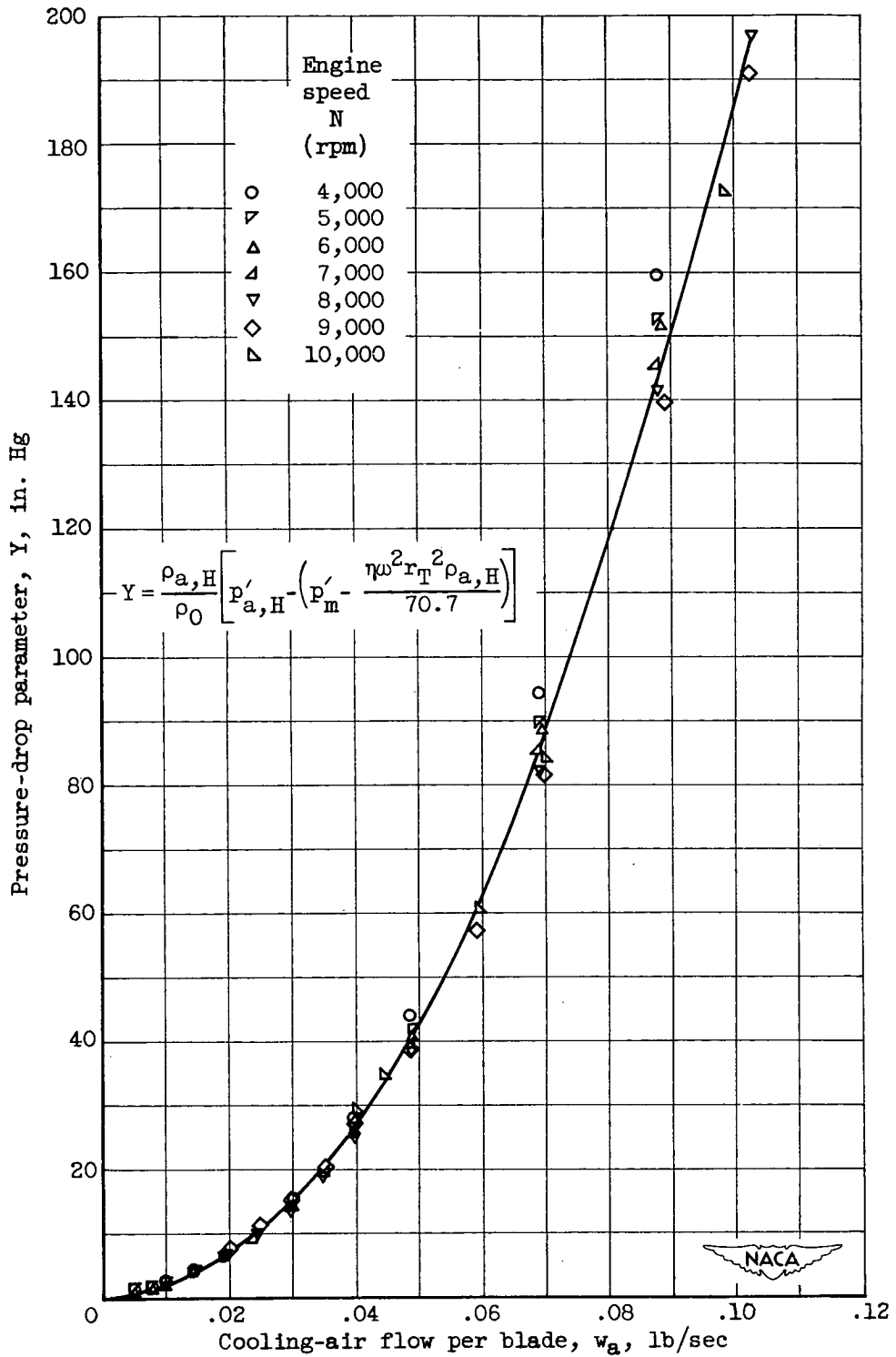
(c) Blades 7 and 8.

Figure 17. - Continued. Correlation of cooling-air-pressure
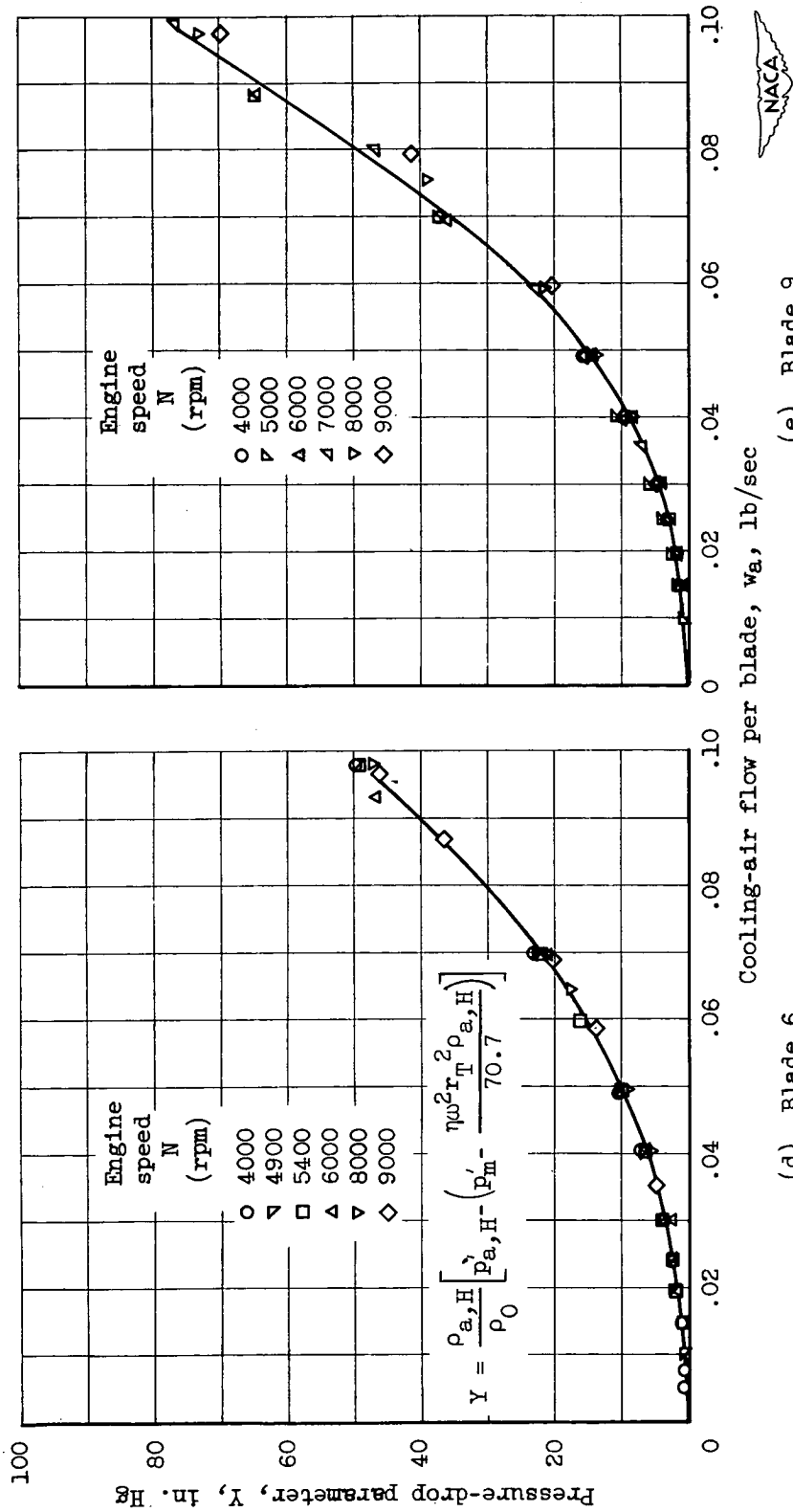drop from rotor hub to blade tip.

$$Y = \frac{\rho_{a,H}}{\rho_0}\left[p'_{a,H} - \left(p'_m - \frac{\eta\omega^2 r_T^2 \rho_{a,H}}{70.7}\right)\right]$$

(d) Blade 6.

(e) Blade 9.

Figure 17. - Concluded. Correlation of cooling-air-pressure drop from rotor hub to blade tip.

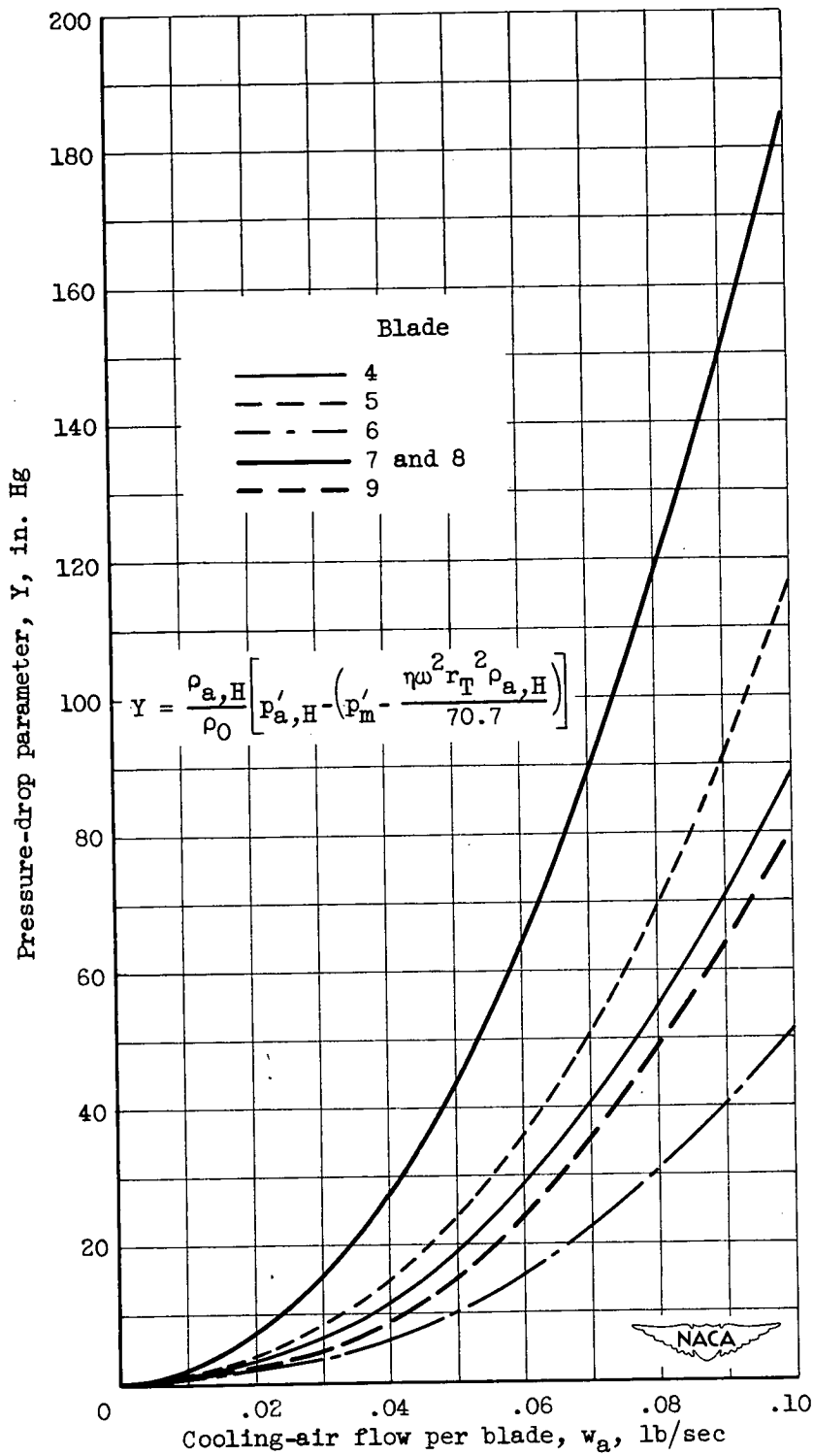Figure 18. - Comparison of cooling-air-pressure drop
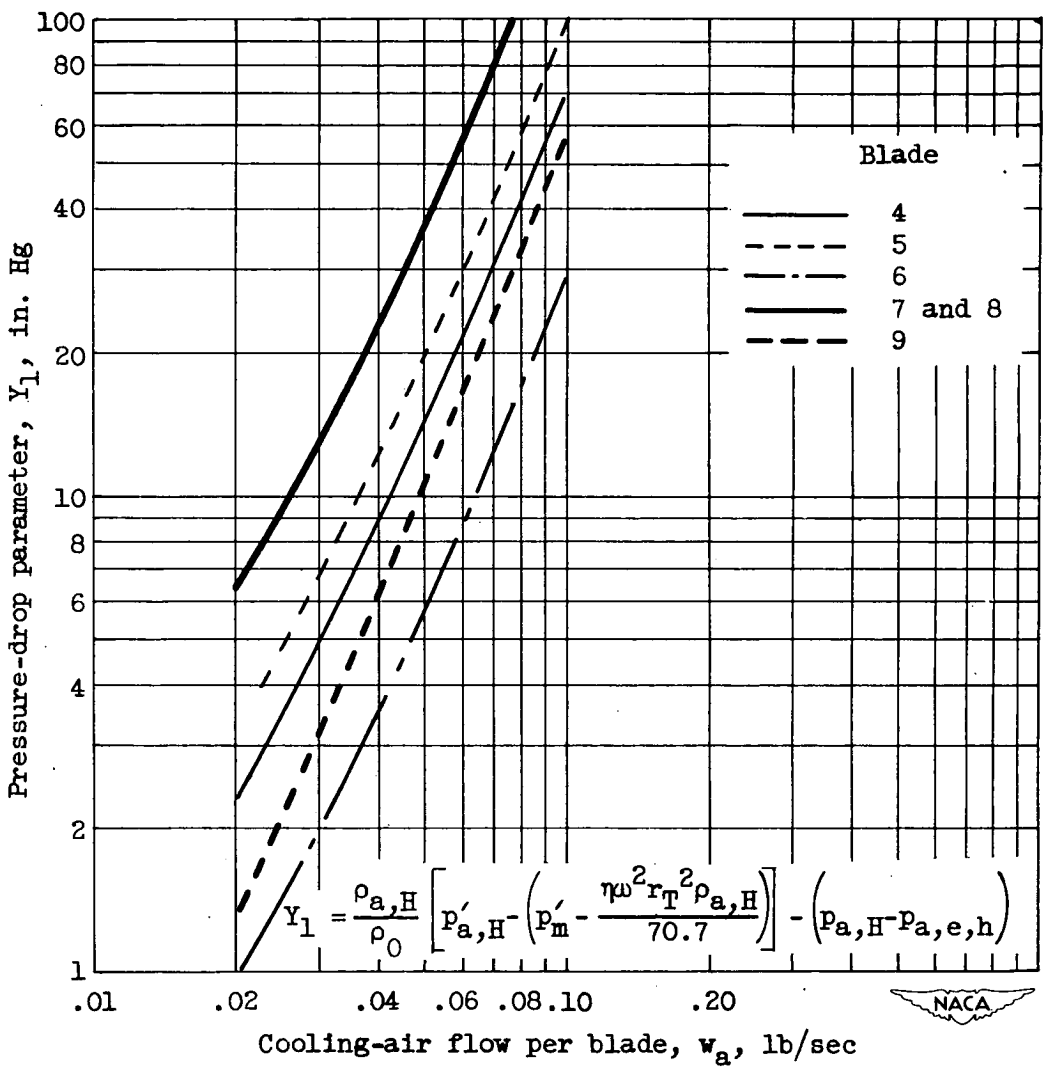from rotor hub to blade tip for blades investigated.

Figure 19. - Comparison of cooling-air-pressure drop from root
to tip of blades investigated.